

000 001 002 003 004 005 006 007 008 009 010 011 012 013 014 015 016 017 018 019 020 021 022 023 024 025 026 027 028 029 030 031 032 033 034 035 036 037 038 039 040 041 042 043 044 045 046 047 048 049 050 051 052 053 REASONING-ALIGNED PERCEPTION DECOUPLING FOR SCALABLE MULTI-MODAL REASONING

Anonymous authors

Paper under double-blind review

ABSTRACT

Recent breakthroughs in reasoning language models have significantly advanced text-based reasoning. On the other hand, Multi-modal Large Language Models (MLLMs) still lag behind, hindered by their outdated internal LLMs. Upgrading these is often prohibitively expensive, as it requires complete vision-language alignment retraining which is costly. To address this issue, we introduce **Perception-Reasoning Decoupling**, which modularizes the MLLM’s reasoning component and makes it easily replaceable. This approach redefines the MLLM’s role to convert multi-modal inputs into detailed textual outputs that can be processed by any powerful, external, text-only LLM reasoners. To align the MLLM’s perceptual output with the final reasoning task, we propose a novel reinforcement learning algorithm called **Visual Perception Optimization** (VPO). VPO rewards the MLLM based on the correctness of answers generated by the external reasoner to produce faithful and query-relevant captions. Together, this decoupling pipeline and VPO form our **Reasoning-Aligned Perception Decoupling** (RAPID) approach. Empirical results show that RAPID achieves significant performance gains on multi-modal reasoning benchmarks. Crucially, RAPID enables a **novel inference-time scaling paradigm**: Once trained with VPO, the MLLM can be paired with any state-of-the-art LLM reasoner for consistent performance improvement without retraining. The implementation of our method is available at: <https://anonymous.4open.science/r/RAPID2-80CD/>.

1 INTRODUCTION

Recent reasoning language models, such as OpenAI-o1 (Jaech et al., 2024) and Qwen3 (Yang et al., 2025a), have driven significant gains in complex math and science tasks. By emulating a deliberate, step-by-step reasoning process akin to human reflection, these models avoid superficial shortcuts. As a result, they substantially outperform previous models like GPT-4o (Hurst et al., 2024), with improvements exceeding 30% on math benchmarks like AIME24 (AIME, 2024) and around 10% on science benchmarks like GPQA (Rein et al., 2024).

Translating breakthroughs from the uni-modal text to the multi-modal domain remains a significant challenge. Existing multi-modal large language models (MLLMs), like Qwen2.5-VL (Bai et al., 2025), Gemma3 (Team et al., 2025a), and InternVL3 (Zhu et al., 2025), still struggle with reasoning and math-intensive tasks because their underlying LLMs are outdated or lack slow-thinking capabilities. While approaches like VL-Rethinker (Wang et al., 2025a) and MM-EUREKA (Meng et al., 2025) try to improve performance with reinforcement learning, their success is fundamentally restricted by the reasoning capability of the base LLM. The ideal solution, namely, switching the LLM with the most state-of-the-art one, is often prohibitive, as it requires repeating the entire, costly vision-language alignment process. This raises the critical question: *Can we replace the LLM within an MLLM to unlock advanced reasoning¹ efficiently, without undertaking redundant vision-language retraining?*

To address that, we propose the **Perception-Reasoning Decoupling** pipeline, where we re-focus the MLLM’s primary role on *perception*. It first translates the multi-modal inputs into a comprehensive textual representation, which is then processed by a separate, powerful, external LLM for *reasoning*. This decoupling allows flexible alteration of the LLM reasoner, offering a path to circumvent the costly retraining cycle. Our key distinction from similar two-stage pipelines (Tiong et al., 2022; Guo et al., 2022; Hu et al., 2022; Gou et al., 2024; Lu et al., 2025) lies in the textual representation, which includes both a *query-relevant caption* and a *tentative solution* to ensure all essential visual

¹In this paper, we focus on multi-modal math and science reasoning tasks.

054 information is captured for subsequent reasoning. However, the critical challenge in this new pipeline
 055 is that *the generated textual outputs are not optimized for correct reasoning*.
 056

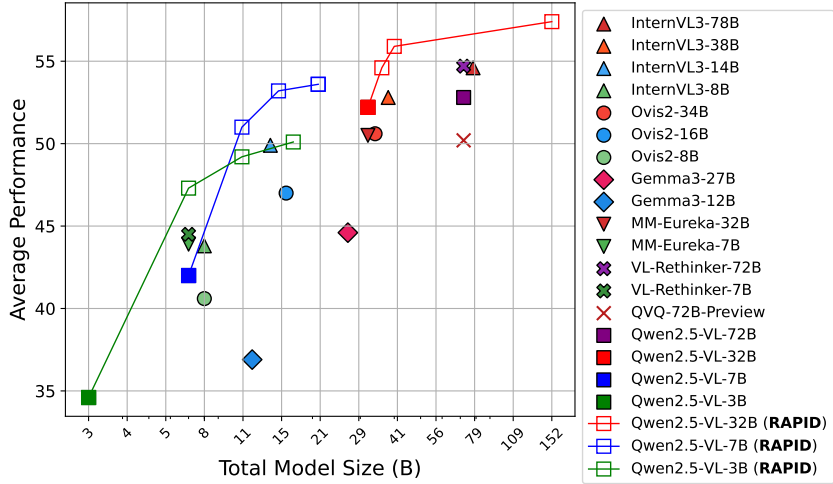


Figure 1: **Comparisons on multi-modal reasoning benchmarks** on average performance and total model size between RAPID-enhanced Qwen2.5-VL series of models and the other existing MLLMs. Check the detailed numerical results in Appendix B and experimental settings in Sec. 4.1.

To overcome that, we introduce **Visual Perception Optimization** (VPO), a novel policy gradient algorithm operating through a reinforcement learning feedback loop where, given a user query, the MLLM first generates a group of query-relevant captions, which are then considered as contexts for the external LLM reasoner to generate final answers. With a correctness-based reward function, the perceptual MLLM is aligned with the reasoning objective, and guided to generate faithful and query-relevant captions optimized for the correctness of downstream reasoning. The combination of the *Perception-Reasoning Decoupling* pipeline with the *VPO algorithm* forms our overall approach, named Reasoning-Aligned Perception Decoupling (RAPID)

Empirically, RAPID achieves notable performance gains on challenging benchmarks such as MathVerse (Zhang et al., 2024), MathVision (Wang et al., 2024b) and LogicVista (Xiao et al., 2024). Moreover, as perception and reasoning are decoupled, the MLLMs trained with VPO generate textual outputs that can be directly fed to any LLM for reasoning. This eliminates the necessity for retraining, and enables RAPID to be a practical solution for the rapid evolution of MLLMs and reasoning LLMs. Figure 1 compares various MLLMs against the RAPID-enhanced Qwen2.5-VL series. For each RAPID-enhanced group (e.g., Qwen2.5-VL-3B), we optimize the MLLM with VPO using minimal data (39K). The resulting performance curves are generated simply by pairing the optimized MLLM with increasingly powerful external LLMs (see Appendix B for the choice of configurations), demonstrating a novel inference-time scaling paradigm.

Our contributions can be summarized as follows:

- We introduce the **Perception-Reasoning Decoupling** pipeline, which redefines MLLMs’ focus to multi-modal perception, allowing the reasoning component to be flexibly replaced by any advanced external LLM without burdensome retraining.
- We propose **Visual Perception Optimization** (VPO), a novel policy gradient algorithm that aligns the MLLM’s perceptual outputs by using the correctness of the external LLM’s final answers with the perceptual outputs as contexts for reward signals.
- Combining both, RAPID achieves significant performance gains and introduces an efficient, novel “plug-and-play” inference-time scaling approach. By eliminating the costly retraining required by traditional methods, an one-time optimized MLLM can be paired with any stronger LLM for continual performance improvements, as demonstrated in Figure 1.

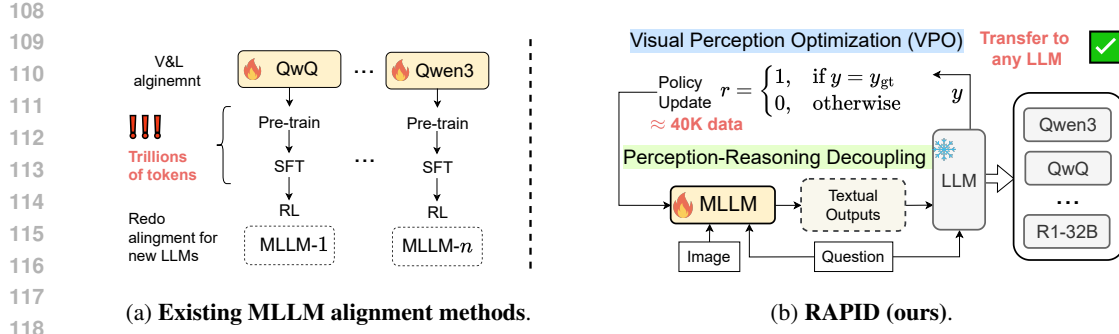


Figure 2: **Comparisons between RAPID and existing alignment methods for reasoning MLLMs.** For novel LLMs, existing methods (a) repeatedly conduct the compute-intensive alignment procedure, while (b) RAPID decouples the *visual perception* from *text-only reasoning* (Sec. 3.1) by learning to extract reasoning-aligned visual contexts with the proposed VPO algorithm (Sec. 3.2). Note that the caption penalty, as in Eq. 3, is omitted here for simplicity. The **flame** and **snowflake** icons indicate the models are trainable and frozen, respectively, during the process.

2 RELATED WORK

Improving the Reasoning Ability of MLLMs. Start with an existing MLLM (*e.g.*, Qwen2.5-VL (Bai et al., 2025)), a widely adopted approach is to perform reinforcement learning or knowledge distillation. For example, VL-Rethinker (Wang et al., 2025a), MM-EUREKA (Meng et al., 2025) and NoisyRollout (Liu et al., 2025a) apply GRPO (Shao et al., 2024) (or its variant (Liu et al., 2025c)) to MLLMs to learn deliberate reasoning patterns. Distillation-based methods, such as R1-OneVision (Yang et al., 2025b), Vision-R1 (Huang et al., 2025) and ReVisual-R1 (Chen et al., 2025a) perform supervised fine-tuning (SFT) on reasoning data. However, both methods are restricted by the base LLMs (*e.g.*, Qwen2.5 (Yang et al., 2024)), which lags behind state-of-the-art reasoning models (*e.g.*, Qwen3-8B (Yang et al., 2025a)). While adopting a stronger LLM is an intuitive solution, re-aligning vision and language through full retraining on trillions of tokens is prohibitively costly.

Caption-then-Reason Pipelines. To leverage LLM reasoning without intensive retraining, prior work explores similar “caption-then-reason” pipelines that decouple perception from reasoning. These approaches use Vision-Language Models (VLMs) (Radford et al., 2021; Li et al., 2022; Yu et al., 2022) or MLLMs for the perception task, while a separate LLM handles reasoning. Efforts in this area primarily focus on improving caption generation, for instance by selecting query-relevant image patches for captioning (Tiong et al., 2022; Guo et al., 2022), prompting MLLMs for query-aware captions (Gou et al., 2024), or enhancing captioning datasets (Hu et al., 2022; Lu et al., 2025). RAPID differs from these works in two key aspects. First, it includes a tentative solution in its generated output to better capture critical visual information. Second, while existing methods do not optimize captions for the final outcome, RAPID rewards the captioning process based on the correctness of the final answer produced by the reasoning LLM.

3 METHODOLOGY

This section describes the two main components of RAPID: *perception-reasoning decoupling* (Sec. 3.1) and *visual perception optimization* (Sec. 3.2). Figure 2 gives an overview of the approach.

3.1 PERCEPTION-REASONING DECOUPLING

Given an image I and a relevant query q , our perception-reasoning decoupling pipeline involves two consecutive stages: (i) **Perception**, where an MLLM (*e.g.*, Qwen2.5-VL (Bai et al., 2025)) acts as a perception module to generate a group of textual outputs O_p (detailed below) with respect to the image I and a perception prompt. (ii) **Reasoning**, where a powerful text-only LLM reasoner (*e.g.*, R1-Distilled-7B (Guo et al., 2025) or Qwen3-8B (Yang et al., 2025a)) receives the original query q and a consolidated set of perceptual outputs, O_p , which are structured by a reasoning prompt P_r (shown in Fig. 12): $y = \text{LLM}(P_r(q, O_p))$. A key advantage of this decoupling pipeline is that the textual outputs form a universal interface between perception (MLLMs) and reasoning (LLMs). This allows the reasoning LLMs to be upgraded independently, boosting performance without the necessity to retrain the MLLMs or alignment. A detailed empirical analysis is provided in Sec. 4.3.

162 **Strategies for Visual Perception O_p .** We explore strategies to generate precise perceptual outputs for reasoning:
 163 • **none**: An empty set of perceptual outputs O_p , which
 164 serves as the control reference group.
 165 • **cap** (Lu et al., 2025): A holistic image caption $o_{\text{cap}} =$
 166 $\text{MLLM}(I, P_{\text{cap}})$ with the template P_{cap} in Fig. 13.
 167 • **qcap** (Gou et al., 2024): A query-relevant caption
 168 $o_{\text{qcap}} = \text{MLLM}(I, P_{\text{qcap}}(q))$ with P_{qcap} in Fig. 14.
 169 • **sol**: A tentative solution $o_{\text{sol}} = \text{MLLM}(I, P_{\text{sol}}(q))$
 170 with the template P_{sol} in Fig. 15, which is “tentative”
 171 as it acts as contexts for LLMs instead of final answers.
 172

173 To evaluate how different compositions of the perceptual
 174 output set O_p affect performance, we perform an experiment on seven multi-modal reasoning
 175 benchmarks (details in Sec. 4.1 for details). In particular, we set O_p to: (i) none; (ii) $\{o_{\text{cap}}\}$; (iii)
 176 $\{o_{\text{qcap}}\}$; (iv) $\{o_{\text{sol}}\}$; (v) $\{o_{\text{cap}}, o_{\text{sol}}\}$; and (vi) $O_p = \{o_{\text{qcap}}, o_{\text{sol}}\}$. The reasoning prompt P_r (shown in
 177 Fig. 12) is designed to provide a unified structure for all the above cases. We use Qwen2.5-VL-7B
 178 for perception and adopt Qwen3-8B and R1-Distilled-7B (referred to as R1-7B) for reasoning. Figure
 179 Figure 3 shows the average accuracies obtained. As can be seen,
 180

181 • **Holistic captions outperform their query-relevant counterparts.** This can be attributed to
 182 the MLLM’s extensive training on holistic image captioning tasks (Bai et al., 2025), whereas
 183 query-relevant captioning remains less optimized. However, with proper optimization (Sec. 3.2),
 184 query-relevant captioning can offer an advantage by extracting contextually relevant visual details.
 185 • **Combining tentative responses and holistic captions achieves best results**, delivering significant
 186 improvement (+7% w/ Qwen3-8B) over the original MLLM. This success is due to the complemen-
 187 tary roles played by the caption and tentative response in reasoning. The caption provides the LLM
 188 with essential contexts for problem-solving, while the tentative response serves as a reference.
 189

190 While Figure 3 shows that cap+sol performs best, we will adopt qcap+sol as the default in the
 191 sequel. The reason is empirical. Our findings in Section 4.2 reveal that qcap+sol outperforms
 192 cap+sol once VPO (to be introduced in Section 3.2) is applied. This indicates that the query-
 193 relevant approach, while less optimized initially, possesses greater potential.
 194

195 3.2 VISUAL PERCEPTION OPTIMIZATION (VPO) 196

197 Although the combination of caption and tentative solution (*i.e.*, both cap+sol and qcap+sol)
 198 demonstrates superior results in Figure 3, they are not optimized for the correctness of the final
 199 reasoning outcome. In other words, the MLLM generates its perception outputs without any feedback
 200 on whether these outputs actually guide the reasoning LLM to the correct answer. To address this
 201 limitation, we introduce **Visual Perception Optimization** (VPO). As illustrated in Figure 4, VPO
 202 establishes a reinforcement learning feedback loop that fine-tunes the MLLM for better captioning,
 203 explicitly rewarding it based on the correctness of the final answer produced by the reasoning LLM.
 204

205 **Objective Design.** Without the loss of generality, we describe VPO using the query-relevant caption
 206 (qcap) setting. VPO is inspired by Group Relative Policy Optimization (GRPO) (Shao et al., 2024),
 207 a policy optimization algorithm originally developed for text-only LLMs. In our setting, the policy
 208 π_θ to optimize is the MLLM performing visual captioning. For a given input pair (I, q) from the
 209 training set p_D , the old policy generates G caption rollouts $\{o^2 \sim \pi_{\theta_{\text{old}}}(I, P_{\text{qcap}}(q))\}$. Let R_i be the
 210 reward for the i th rollout. The normalized advantage is $\hat{A}_i = \frac{R_i - \bar{R}}{\sigma(R)}$, where $\sigma(R)$ is the standard
 211 deviation of rewards within the group $R = \{R_i\}$ and $\bar{R} = \frac{1}{G} \sum_{i=1}^G R_i$ is the baseline reward. Thus,
 212 the objective of VPO, following the formulation of GRPO, can be represented as:
 213

214
 215 ²Here, we denote o_i as the query-relevant captions qcap , rather than holistic captions cap or tentative
 216 solutions sol , as in Sec. 3.1

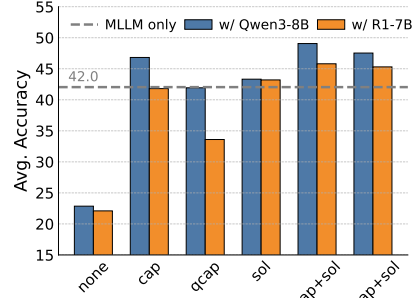


Figure 3: Comparison of the strategies for visual perception O_p .

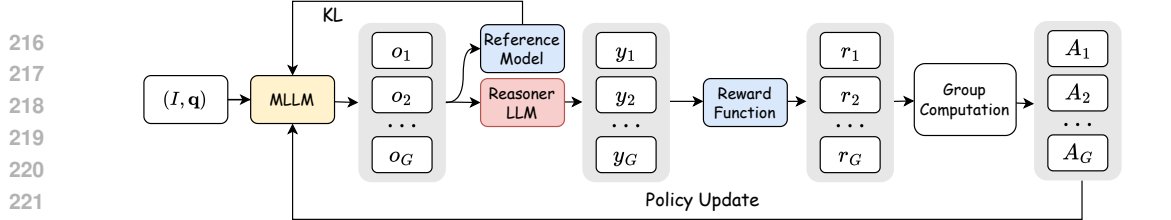


Figure 4: **Visual Perception Optimization (VPO)** reinforces *captions* that induce correct *reasoning* results via reinforcement learning with verifiable rewards. Here we omit caption penalty for simplicity.

$$L(\theta) = \mathbb{E}_{(I, q) \sim p_{\mathcal{D}}, o \sim \pi_{\theta_{\text{old}}}(\cdot | I, P_{\text{qcap}}(q))}$$

$$\left[\frac{1}{G} \sum_{i=1}^G \min \left(\frac{\pi_{\theta}(o_i | I, P_{\text{qcap}}(q))}{\pi_{\theta_{\text{old}}}(o_i | I, P_{\text{qcap}}(q))} \hat{A}_i, \text{clip} \left(\frac{\pi_{\theta}(o_i | I, P_{\text{qcap}}(q))}{\pi_{\theta_{\text{old}}}(o_i | I, P_{\text{qcap}}(q))}, 1 - \epsilon_l, 1 + \epsilon_h \right) \hat{A}_i \right) \right], \quad (1)$$

which incorporates a surrogate loss clipped to $[1 - \epsilon_l, 1 + \epsilon_h]$ ($\epsilon_l > 0, \epsilon_h > 0$) and a KL-penalty $D_{\text{KL}}[\pi_{\theta} || \pi_{\theta_{\text{ref}}}]$ weighted by β (not shown) to stabilize optimization.

Reward Design. GRPO is often used in math reasoning problems (Shao et al., 2024; Guo et al., 2025), in which the reward is determined by a simple rule because the model’s output is the final solution itself. However, in our setting, the MLLM generates an intermediate caption, from which the reasoning solution cannot be directly extracted. To address this, for each caption rollout o_i , we prompt the reasoning LLM to generate a final answer, and the reward is determined by whether this answer matches the ground-truth. This is formalized as follows:

$$\hat{R}_i = r(y_{\text{gt}}, y_i) = \mathbb{1}(y_{\text{gt}} = \text{parse}(y_i)), \quad \text{where } y_i = \text{LLM}(P'_{\text{reason}}(q, o_i)), \quad (2)$$

where y_i is the answer produced by the LLM from caption o_i , $\mathbb{1}(\cdot)$ is the indicator function, and $P'_{\text{reason}}(q, o_i)$ (shown in Figure 16) is the reasoning prompt different from that used for inference (template in Figure 12) as it omits the tentative solution. The reward function $r(\cdot, \cdot)$ compares the predicted answer with the ground-truth y_{gt} .

During training, we observe reward hacking (details in Sec. 4.2), where the MLLM directly solves the problem instead of performing captioning. Consequently, the model’s captioning ability does not improve. To address that, we impose a penalty on reward \hat{R}_i if (i) o_i leads to a correct answer; and (ii) o_i does not contain a caption (determined by the policy MLLM π_{θ} via few-shot prompting):

$$R_i = \hat{R}_i - \lambda \mathbb{1}(\hat{R}_i = 1 \wedge \text{hasCap}(o_i)), \quad (3)$$

where, λ is a penalizing factor, and $\text{hasCap}(\cdot)$ ³ checks if o_i contains a caption (template in Figure 17).

In summary, VPO offers two primary advantages:

- **Generation of Reasoning-Aligned Captions:** VPO uses the final reasoning outcome as a reward signal to optimize MLLMs, ensuring the captions are not merely descriptive but also functionally aligned for further reasoning. Check the quality improvement we demonstrate in Sec. 4.4.
- **LLM-Agnostic and Generalizable Improvement:** VPO is an LLM-agnostic optimization, *i.e.*, the optimized MLLMs communicate with the LLM reasoners via natural languages, and thus, the performance gains are generalizable across any LLMs. This enables a **one-time alignment**, which can be paired with any LLMs in a plug-and-play way without repeating VPO, as shown in Sec. 4.3.

In addition to captions, we further improve the quality of the tentative solution generated by the MLLM. As the tentative solution can be easily verified by a rule-based reward function, we apply GRPO on the MLLM. Details can be found in Appendix D. In the experiments, we optimize the MLLM with GRPO and VPO in a sequential manner, with VPO followed by GRPO.

4 EXPERIMENTS

4.1 MAIN RESULTS

Baselines. We compare our method with the following baselines: (i) Proprietary models, including Claude-3.7-Sonnet (Anthropic, 2025), Gemini-2.0-Flash (DeepMind, 2025) and GPT-4o (Hurst

³We evaluate this check function and consider other variants in Appendix E.3.

Table 1: **Comparison on multi-modal reasoning benchmarks** with respect to average accuracies. The best results are **bold**, while the second best are underlined. *: short for GPT-OSS-120B-A5B. ‡: undergone GRPO training.

Model	MathVista	MathVision	MathVerse	MMMU	WeMath	DynaMath	LogicVista	AVG
Proprietary Models								
Open-Source Models								
Claude-3.7-Sonnet	66.8	41.9	46.7	75.0	49.3	<u>39.7</u>	58.2	53.9
Gemini-2.0-Flash	70.4	43.6	47.7	<u>72.6</u>	47.4	42.1	52.3	53.7
GPT-4o-20241120	60.0	31.2	40.6	<u>70.7</u>	45.8	34.5	52.8	47.9
Verification-augmented and Tool-enabled MLLMs								
Qwen2.5-VL-7B [‡] (Bo8)	76.8	31.6	46.8	58.1	43.1	29.7	48.6	47.8
SRPO-7B	<u>75.8</u>	32.9	-	<u>57.1</u>	-	-	-	-
ReVPT-7B	66.0	-	-	-	-	-	-	-
DeepEyes-7B	70.1	26.6	47.3	-	38.9	-	47.7	-
Prior Caption-then-Reason Methods								
ECSO	64.6	42.7	42.8	61.4	38.4	25.0	39.4	44.9
OmniCaptioner	67.5	43.3	48.0	62.2	38.7	30.5	56.2	49.5
Qwen2.5-VL series and our RAPID-enhanced counterparts								
Qwen2.5-VL-3B	64.5	21.9	28.8	50.1	24.2	13.4	39.6	34.6
w/ RAPID (Qwen3-8B)	69.6	40.8	48.6	60.9	39.1	29.3	56.4	49.2
Qwen2.5-VL-7B	70.3	25.8	41.0	57.3	34.4	19.4	46.1	42.0
w/ RAPID (Qwen3-8B)	76.1	43.7	52.2	64.7	45.4	32.7	57.7	53.2
Qwen2.5-VL-32B	76.8	37.8	50.1	69.0	43.1	33.3	55.0	52.2
w/ RAPID (Qwen3-8B)	76.8	47.0	54.4	67.8	48.5	36.5	60.4	55.9
w/ RAPID (GPT-A5B)*	75.9	<u>52.1</u>	54.3	69.8	50.8	38.3	60.4	57.4
Qwen2.5-VL-72B	74.2	39.3	47.3	68.2	49.1	35.9	55.7	52.8
w/ RAPID (GPT-A5B)*	75.1	53.4	56.2	72.4	52.1	37.9	59.1	58.0

et al., 2024); (ii) Open-source general-purpose MLLMs, including Qwen2.5-VL (3B/7B/32B/72B) (Bai et al., 2025), InternVL3 (8B/14B/38B/78B) (Zhu et al., 2025), Gemma-3 (12B/27B) (Team et al., 2025a) and Ovis2 (8B/16B/34B) (Lu et al., 2024b); (iii) Open-source MLLMs specialized for reasoning, including MM-Eureka (7B/32B) (Meng et al., 2025), VL-Rethinker (7B/72B) (Wang et al., 2025a), QVQ-72B-Preview (Qwen, 2024) and ReVisual-R1-7B (Chen et al., 2025a). (iv) Latest Caption-then-Reason pipelines, such as ECSO (Gou et al., 2024) and OmniCaptioner (Lu et al., 2025). We use the GRPO-optimized Qwen2.5-VL-7B as captioner and Qwen3-8B as the reasoner; (v) Qwen2.5-VL-7B[‡] (Bo8) that performs best-of-8 verification with VisualPRM-8B-v1.1 (Wang et al., 2025b), SRPO-7B (Wan et al., 2025) that conducts self-verification, ReVPT-7B (Zhou et al., 2025) and DeepEyes-7B (Zheng et al., 2025) that call tools for better perception.

Evaluation is conducted on a diverse set of multi-modal reasoning benchmarks, *e.g.*, MathVista (testmini) (Lu et al., 2024a), MathVision (test) (Wang et al., 2024b), MathVerse (vision-only) (Zhang et al., 2024), MMMU (val) (Yue et al., 2024), WeMath (Qiao et al., 2024), DynaMath (Zou et al., 2024), and LogicVista (Xiao et al., 2024). As in recent works (Wang et al., 2025c; Zhu et al., 2025), we use VLMEvalKit (Duan et al., 2024) for evaluation, and report the worst-case accuracy for DynaMath, the strict accuracy for WeMath, and overall accuracy for the other benchmarks.

Table 2: **Ablation study of different components of RAPID** (with Qwen2.5-VL-7B by default). VPO[†]: VPO without the caption penalty; [‡]: using `cap+sol` for reasoning-perception decoupling.

	Decouple	GRPO	VPO [†]	Cap. penalty	Math Vista	Math Vision	Math Verse	MMMU	We Math	Dyna Math	Logic Vista	AVG
Ⓐ					70.3	25.8	41.0	57.3	34.4	19.4	46.1	42.0
Ⓑ	✓				70.0	40.4	45.2	62.0	39.1	26.3	49.7	47.5
Ⓒ	✓	✓			72.7	43.2	50.0	63.3	41.1	28.7	54.1	50.5
Ⓓ	✓	✓	✓		76.0	41.5	50.6	62.9	43.1	33.1	57.7	52.2
Ⓔ	✓	✓	✓	✓	76.1	<u>43.7</u>	52.2	64.7	45.4	32.7	<u>57.7</u>	53.2
Ⓕ	✓ [‡]	✓	✓	✓	71.2	43.8	48.1	64.6	39.9	32.3	57.9	51.1
Ⓖ	✓		✓	✓	74.2	42.5	<u>50.8</u>	62.0	39.4	31.9	56.6	51.1
Ⓗ		✓			74.2	29.7	44.8	55.9	41.0	27.7	48.1	45.9
Ⓘ	✓	✓	✓		75.0	29.8	42.0	55.8	40.8	23.0	46.3	44.7

Implementation Details of RAPID. We perform RAPID upon the Qwen2.5-VL series (3B, 7B, 32B, and 72B) MLLMs. During training, we use R1-Distilled-7B (R1-7B) as the reasoner to compute reward signals for all MLLMs. During evaluation, we adopt Qwen3-8B⁴ (Yang et al., 2025a) and GPT-OSS-120B (Agarwal et al., 2025) as the LLM reasoners. For training data, we adopt ViRL39K (Wang et al., 2025a), a curated dataset of 38,870 verifiable multi-modal question-answer pairs tailored for multi-modal reasoning. We implement GRPO and VPO with verl (Sheng et al., 2025) with a global batch size of 256, a rollout temperature of 1.0, and a learning rate of $1e^{-6}$.

Implementation Details of GRPO. We set the number of rollouts to 8 for the 3B/7B MLLMs and 4 for the 32B/72B MLLMs. Following Yu et al. (2025), we remove KL regularization and use the "Clip-Higher" strategy, setting ϵ_l to 0.2 and ϵ_h to 0.25. When reporting performance with GPRO but without VPO (e.g., Ⓜ and ⓪ in Table 2 or the baselines in Table 3), we select the best-performing checkpoints (with perception-reasoning decouple applied) at 400, 300, and 100 steps for the 3B, 7B, and 72B MLLMs, respectively, based on the average accuracies across the seven reasoning datasets (evaluated every 50 steps). GRPO is not applied to the 32B variant, as it has already been RL-tuned.

Implementation Details of VPO. We set the number of rollouts to 4, KL-penalty coefficient β to e^{-3} , and penalizing constant λ in Eq. (3) to 0.1. VPO is applied to the MLLM following 200 steps of GRPO⁵ (except for the 32B model, which we directly use the original model). Similar to GRPO, we select the best checkpoints at 200, 150, 100, and 100 for the 3B, 7B 32B, and 72B models according to their average accuracies on the reasoning datasets.

Results. Table 1 compares the performance of RAPID and baseline MLLMs on seven multi-modal reasoning datasets. It highlights two merits of RAPID: (i) **It achieves significant performance gains on the reasoning tasks compared to the original MLLMs.** For example, applying RAPID to Qwen2.5-VL-7B with a similar-sized LLM (Qwen3-8B) yields an average accuracy of 53.2% (+11.2% compared to the original MLLM). Notably, when applying RAPID to Qwen2.5-VL-72B with GPT-OSS-120B as the LLM, we achieve the best average accuracy of 58% across all the models compared, even surpassing proprietary MLLMs. (ii) **RAPID achieves better performance-size trade-off.** For example, Qwen2.5-VL-7B with RAPID (Qwen3-8B) with a total size of 15B outperforms larger models such as MM-Eureka-32B, InternVL3-38B and Ovis2-34B. Similarly, Qwen2.5-VL-32B with RAPID (Qwen3-8B) surpasses VL-Rethinker-72B and InternVL3-78B. Check Figure 1 for a better visualization of the performance-size trade-off. More analysis on the **training and inference compute efficiency** is provided in Appendix E. (iii) **RAPID surpasses latest caption-then-reason methods** (Gou et al., 2024; Lu et al., 2025), mainly due to the usage of tentative responses and VPO.

Evaluation on General Benchmarks Although RAPID is specifically designed for multi-modal math and science reasoning, we verify that it does not hurt general abilities. We evaluated the VPO/GRPO-optimized Qwen2.5-VL-7B on general benchmarks in a "non-thinking" mode, per common protocols (Yang et al., 2025a; Wang et al., 2025d). As shown in Figure 5, its performance remains on par with the original model. This confirms that our method is a targeted enhancement for reasoning that preserves the model's general abilities. (Benchmark details and Qwen2.5-VL-3B results are in Appendix F.1).

⁴We do not use R1-7B as we found the similar-sized Qwen3-8B performs better in Sec. 4.3.

⁵For the 3B model, we observe that training with VPO after GRPO results in slight forgetting of reasoning. To mitigate this, we switch back to GRPO optimization for an additional 100 steps after VPO.

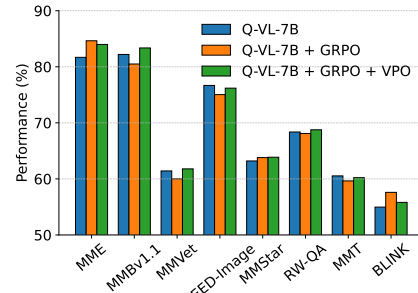


Figure 5: **General benchmark Results.**

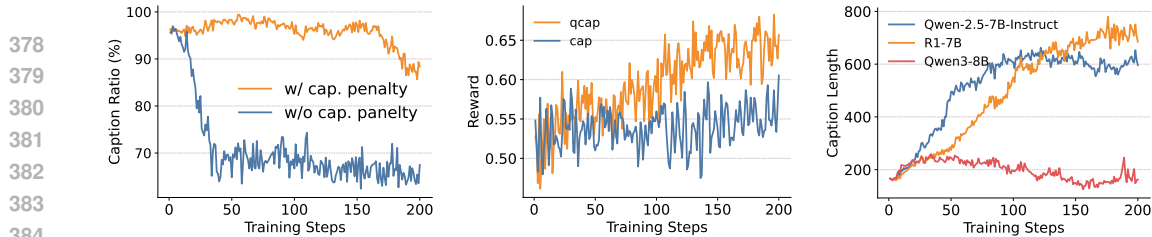


Figure 7: **Reward hacking without the caption penalty.** Figure 8: **Reward dynamics of adopting qcap and cap.** Figure 9: **Caption length trend with various LLMs.**

4.2 ABLATION STUDIES

In this section, we first investigate the effectiveness of the proposed components, *i.e.*, reasoning-perception decoupling (denoted “Decouple”) and VPO. For VPO, we ablate the choices on reward computation during training. Next, we assess the generalization and scalability of RAPID to different LLMs. We use the same training configurations as in Sec. 4.1. Qwen2.5-VL-3B/7B are adopted for ablations due to resource constraints. Unless otherwise specified, we use R1-7B as the default LLM for training (reward computation) and Qwen3-8B for inference.

Reasoning-Perception Decoupling & VPO. Table 2 presents a detailed ablation study of RAPID’s with the 7B MLLM (see Appendix F.2 for the 3B MLLM), which we analyze by incrementally adding each one to the baseline. Starting from the baseline MLLM (Ⓐ), we first apply **perception-reasoning decoupling**. This step alone (Ⓑ) yields a significant 5.5% average improvement, demonstrating the immediate benefit of leveraging a stronger external LLM (Qwen3-8B) for reasoning. Building on this, we apply **GRPO** to enhance the MLLM’s perception by optimizing its tentative solutions, which adds another 3.0% to the average score (Ⓒ). We then apply **VPO** without the caption penalty (Ⓓ), and achieves a further 1.7% gain. Finally, incorporating the **caption penalty** leads to our full model (Ⓔ), adding another 1.0%. This brings the total improvement from our full VPO method to 2.7% over the model with only GRPO (Ⓒ). This caption penalty is crucial for VPO’s effectiveness, as it prevents reward-hacking where the model might generate solutions instead of the intended captions. Figure 7 confirms this: without the penalty, the ratio of rollouts containing valid captions diminishes rapidly, whereas with the penalty, it remains stable above 95% before 150 steps.

The results also highlight that GRPO and VPO are complementary, whose synergy is evident in two ways: 1) Removing either method from the full decoupled setup (Ⓐ vs. ⏏, and ⌂ vs. ⏏) results in suboptimal performance, confirming both are necessary. 2) Figure 6 further visualizes this dynamic: after initial gains from GRPO begin to plateau, VPO provides a distinct secondary performance boost. Despite these gains, the decoupling strategy remains the most critical element. An MLLM improved by VPO and GRPO alone (Ⓓ) still lags far behind the decoupled version (Ⓔ), underscoring its importance. We also note that VPO does not improve MLLM’s reasoning capabilities on its own (Ⓕ vs. ⌂); the slight performance drop suggests minor forgetting during sequential training. However, we demonstrate in Appendix E.4 that this issue can be addressed by simple GPRO training without impacting the overall performance of the 7B model.

While holistic captions (cap+sol) initially outperform query-relevant ones (qcap+sol) as discussed in Section 3.1, this trend reverses after applying VPO (see ⏏ and ⏏). We hypothesize that this is because qcap is easier to optimize during VPO, as the query guides the MLLM to focus on relevant visual details. Instead, without such guidance, the MLLM struggles to identify pertinent information for cap. This is confirmed by Figure 8, which shows that training rewards for qcap increase steadily, while rewards for cap oscillate without consistent growth.

Choices on Reward Computation. We study VPO reward computation by varying the reasoning LLM (during training) and its input content. We take the best-performing checkpoint (optimized

432 with GRPO) as the baseline and evaluate under the perception-reasoning decoupled paradigm. First,
 433 we keep the input content as $qcap+sol$ and test three LLMs with increasing reasoning capacity:
 434 Qwen2.5-7B-Instruct (weak), R1-7B (intermediate), and Qwen3-8B (strong), respectively.
 435

436 As shown in Table 3, the R1-7B LLM performs best. We hypothesize this is due to a trade-off in reasoning
 437 capacity, reflected in caption lengths. Figure 9 shows the caption lengths during training for various LLMs.
 438 We speculate that the stronger Qwen3-8B can succeed with succinct captions, thus inadvertently rewarding
 439 short captions that miss details⁶, while the weaker Qwen2.5-Instruct-7B incentivizes overlong captions
 440 that even include inaccurate solutions. R1-7B strikes an effective balance, making it our default choice.
 441

442 Next, we examine the choice of input content: using
 443 caption alone ($qcap$) versus using the caption plus a
 444 tentative solution ($qcap+sol$). As in Table 3, using
 445 only the caption is superior. Including tentative solutions allows the LLM to take a shortcut during
 446 training—relying on the solutions while ignoring captions—which generates a noisy reward signal
 447 ineffective for optimizing caption quality.⁷ **Additionally, we explore fine-tuning the LLM for better**
 448 **reasoning ability in Appendix E.6.**

452 4.3 GENERALIZATION AND SCALING WITH DIFFERENT LLMs.

453 A practical requirement is that our MLLM, once optimized,
 454 should generalize to new, unseen LLMs at inference time
 455 without retraining. To test this, we perform VPO on the
 456 GRPO-trained MLLM using only R1-7B as the LLM for
 457 this optimization step. We then evaluate its performance
 458 against the baseline (the MLLM without VPO) by pairing
 459 both MLLMs with a diverse range of different LLMs at
 460 inference time, as shown in Figure 10. . We have three
 461 observations. *First, the performance gain from VPO generalizes effectively.* The gap between the VPO-trained model
 462 (solid curves) and the baseline (dashed curves) is main-
 463 tained or widened when using stronger LLMs, revealing
 464 that the benefit is not confined to the specific LLM used
 465 for training. *Second, the RAPID’s scalability is evident as absolute performance trends upward when using more*
 466 *capable LLMs, although this improvement is not strictly*
 467 *monotonic with model size.* Additionally, among the LLMs tested, Qwen3-8B strikes the best balance
 468 between performance and model size, establishing it to be our default choice for the inference stage.
 469 Note that the *optimal LLMs for training and inference might differ (c.f., Table 3 and Figure 10).*

472 4.4 EVALUATION ON CAPTION QUALITY

473 We validate the improved quality of the captions generated
 474 by VPO-optimized MLLMs via a pairwise comparisons
 475 (Chen et al., 2023; Liu et al., 2024b) using GPT-4o (Open-
 476 AI, 2024) as a judge. With 1000 random samples per
 477 dataset, GPT-4o compares captions from Qwen2.5-VL-3B
 478 trained with and without VPO. The judge is instructed
 479 to prefer captions with more comprehensive and accurate
 480 details required to answer the question, while excluding
 481 any solving process (the prompt is in Appendix F.3). We
 482 alternate the caption order to mitigate position bias (Zheng
 483 et al., 2023). As shown in Figure 11, the VPO-optimized
 484 MLLM’s captions demonstrate a clear advantage across all datasets, highlighting the VPO’s effec-

485 Table 3: **Ablation studies** on (a) LLM types
 and (b) input to LLM for reward computation.

Configuration	Q-VL-3B	Q-VL-7B
w/o VPO (baseline)	46.1	50.5
<i>(a) LLM Types</i>		
Qwen2.5-7B-Instruct	47.5	51.9
R1-Distilled-7B	47.9	53.2
Qwen3-8B	47.1	51.3
<i>(b) LLM Input Contents</i>		
$qcap+sol$	47.4	49.5
$qcap$	47.9	53.2

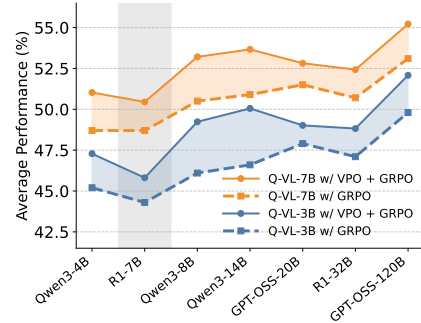


Figure 10: **Performance with different LLMs.** (Only R1-7B is used in training)
 First, the performance gain from VPO generalizes effectively. The gap between the VPO-trained model (solid curves) and the baseline (dashed curves) is maintained or widened when using stronger LLMs, revealing that the benefit is not confined to the specific LLM used for training. Second, the RAPID’s scalability is evident as absolute performance trends upward when using more capable LLMs, although this improvement is not strictly monotonic with model size. Additionally, among the LLMs tested, Qwen3-8B strikes the best balance between performance and model size, establishing it to be our default choice for the inference stage. Note that the optimal LLMs for training and inference might differ (c.f., Table 3 and Figure 10).

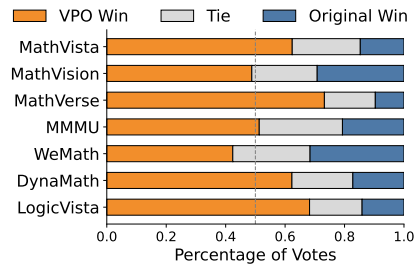


Figure 11: **Pairwise comparison** on the caption quality with and without VPO.

⁶We further validate this in Appendix E.5

⁷Notably, this optimal input format differs from that used in the perception-reasoning decoupling stage.

Table 4: **Effectiveness of different components of RAPID** (with InternVL3-8B by default). VPO[†]: VPO without the caption penalty.

Decouple	GRPO	VPO [†]	Cap. penalty	Math Vista	Math Vision	Math Verse	MMMU	We Math	Dyna Math	Logic Vista	Avg
✓				73.6	29.3	39.8	62.7	37.1	25.5	44.1	44.6
✓	✓			71.3	42.4	39.3	64.4	38.8	29.1	50.1	47.9
✓	✓	✓	✓	73.2	42.6	44.3	64.4	40.2	31.1	52.1	49.7
				75.4	43.2	48.5	64.6	43.2	33.2	55.5	51.9

tiveness (We conduct a case study on caption quality in Appendix I). Moreover, we extend this comparison to other MLLMs and validate these findings with human assessment in Appendix F.3.

4.5 GENERALIZATION ACROSS MLLMs

We confirm RAPID’s generalizability across various MLLMs. Applying decoupling (with Qwen3-8B) and VPO to InternVL3-8B yields significant gains (Table 4), mirroring our main results (Table 2). This suggests that RAPID does generalize across different MLLMs. Moreover, applying the decoupling pipeline alone to more MLLMs (*i.e.*, InternVL3-8B, VL-Rethinker-7B and MM-Eureka-7B) with different LLMs (*i.e.*, Qwen3-8B and GPT-OSS-120B) also shows consistent improvements (Table 17), indicating that decoupling is a broadly effective strategy for enhancing MLLM performance.

4.6 COST ANALYSIS

The section analyzes the cost and time for both the GRPO and VPO training phases. The calculations are based on the publicly listed rental price for NVIDIA H20 GPUs from the cloud provider LuchenTech⁸. The price used for this estimation is approximately \$0.56 per GPU per hour.

Table 5 provides a comprehensive breakdown of the resource requirements and associated costs for training MLLMs of various sizes. As can be seen, our method is remarkably cost-effective, requiring less than 300\$ to obtain significant performance advantages (check Figure 1 and Table 1). This low financial barrier makes the approach highly accessible for a wide range of users, including small research teams, companies, and even individual researchers.

Additionally, as shall be discussed in Appendix E.1, these costs are less than 0.1% of the resource-intensive and often prohibitive expenses required for pre-training or fine-tuning an MLLM with a new LLM, positioning RAPID as a highly practical and efficient alternative.

Table 5: **Training time and cost analysis** for different model sizes and training phases in RAPID.

Model Size	Stage	Wall-Clock Time (hours)	Training Steps	Hardware (GPUs)	GPU Hours	Estimated Total Cost (USD)
3B	GRPO	16.7	200	8 × H20	133.6	\$74.8
	VPO	23.9	200	16 × H20	382.4	\$214.1
7B	GRPO	24.0	200	8 × H20	192.0	\$107.5
	VPO	16.3	150	16 × H20	260.0	\$145.6
32B	VPO	13.6	100	32 × H20	435.2	\$243.7

5 CONCLUSION

This paper proposes RAPID, an efficient method for constructing multi-modal reasoning models. By decoupling visual perception (MLLM) from text-only reasoning (LLM), RAPID leverages the advanced reasoning of frontier LLMs while avoiding burdensome visual re-alignment. Enhanced with Visual Perception Optimization, this method reinforces precise captions to provide rich visual context, improving reasoning and effectively scaling to more advanced LLMs at inference time. Our approach achieves significant accuracy gains on multiple multi-modal reasoning benchmarks while remaining computationally efficient.

⁸<https://www.luchentech.com/>

540
541 ETHICS STATEMENT

542 We affirm that this work adheres to the ICLR Code of Ethics.⁹ Our research does not involve human
 543 subjects, personal data, or sensitive attributes, and it does not pose foreseeable risks of physical,
 544 psychological, or social harm. All datasets used in our experiments are publicly available and widely
 545 adopted in the research community. We have carefully considered potential issues related to bias,
 546 fairness, and misuse, and we believe that the scope of this study does not introduce additional ethical
 547 concerns. Furthermore, our work complies with all relevant legal, institutional, and research integrity
 548 requirements, and we declare that there are no conflicts of interest or competing financial relationships
 549 that could have influenced this research.

550
551 REPRODUCIBILITY STATEMENT
552

553 We have taken extensive steps to ensure the reproducibility of our work. All model architectures,
 554 training procedures, and hyperparameters are described in detail in the main text (Section 3 and
 555 Section 4) and the Appendix. For empirical results, we specify dataset sources and preprocessing
 556 steps in Section 4.1, and we provide implementation details and experimental settings in Section 4.1.
 557 Anonymous source code and scripts for reproducing the main experiments will be made available in
 558 the link provided in the abstract. We believe these efforts enable full reproducibility of our reported
 559 results.

560
561 REFERENCES
562

563 Sandhini Agarwal, Lama Ahmad, Jason Ai, Sam Altman, Andy Applebaum, Edwin Arbus, Rahul K
 564 Arora, Yu Bai, Bowen Baker, Haiming Bao, et al. gpt-oss-120b & gpt-oss-20b model card. Preprint
 565 arXiv:2508.10925, 2025.

566 Pranjal Aggarwal and Sean Welleck. L1: Controlling how long a reasoning model thinks with
 567 reinforcement learning. *arXiv preprint arXiv:2503.04697*, 2025.

568 AIME. AIME problems and solutions, 2024. https://artofproblemsolving.com/wiki/index.php/AIME_Problems_and_Solutions, 2024.

569 Anonymous. SAM 3: Segment anything with concepts. In *Submitted to The Fourteenth International*
 570 *Conference on Learning Representations*, 2025. URL <https://openreview.net/forum?id=r35c1VtGzw>. under review.

571 Anthropic. Claude 3.7 Sonnet System Card. Technical report, 2025. Accessed: 2025-05-16.

572 Shuai Bai, Keqin Chen, Xuejing Liu, Jialin Wang, Wenbin Ge, Sibo Song, Kai Dang, Peng Wang,
 573 Shijie Wang, Jun Tang, Humen Zhong, Yuanzhi Zhu, Mingkun Yang, Zhaohai Li, Jianqiang Wan,
 574 Pengfei Wang, Wei Ding, Zheren Fu, Yiheng Xu, Jiabo Ye, Xi Zhang, Tianbao Xie, Zesen Cheng,
 575 Hang Zhang, Zhibo Yang, Haiyang Xu, and Junyang Lin. Qwen2.5-VL technical report. Preprint
 576 arXiv:2502.13923, 2025. URL <https://arxiv.org/abs/2502.13923>.

577 Kai Chen, Chunwei Wang, Kuo Yang, Jianhua Han, Lanqing Hong, Fei Mi, Hang Xu, Zhengying
 578 Liu, Wenyong Huang, Zhenguo Li, Dit-Yan Yeung, Lifeng Shang, Xin Jiang, and Qun Liu.
 579 Gaining Wisdom from Setbacks: Aligning large language models via mistake analysis. Preprint
 580 arXiv:2310.10477, 2023.

581 Lin Chen, Jinsong Li, Xiaoyi Dong, Pan Zhang, Yuhang Zang, Zehui Chen, Haodong Duan, Jiaqi
 582 Wang, Yu Qiao, Dahua Lin, et al. Are we on the right way for evaluating large vision-language
 583 models? *Advances in Neural Information Processing Systems*, 37:27056–27087, 2024.

584 Shuang Chen, Yue Guo, Zhaochen Su, Yafu Li, Yulun Wu, Jiacheng Chen, Jiayu Chen, Weijie Wang,
 585 Xiaoye Qu, and Yu Cheng. Advancing multimodal reasoning: From optimized cold start to staged
 586 reinforcement learning. Preprint arXiv:2506.04207, 2025a.

587
588
589
590
591
592
593 ⁹<https://iclr.cc/public/CodeOfEthics>

594 Song Chen, Xinyu Guo, Yadong Li, Tao Zhang, Mingan Lin, Dongdong Kuang, Youwei Zhang,
 595 Lingfeng Ming, Fengyu Zhang, Yuran Wang, et al. Ocean-ocr: Towards general ocr application
 596 via a vision-language model. *arXiv preprint arXiv:2501.15558*, 2025b.

597

598 Google DeepMind. Gemini 2.0 Flash. <https://cloud.google.com/vertex-ai/generative-ai/docs/models/gemini/2-0-flash>, 2025.

599

600 Haodong Duan, Junming Yang, Yuxuan Qiao, Xinyu Fang, Lin Chen, Yuan Liu, Xiaoyi Dong, Yuhang
 601 Zang, Pan Zhang, Jiaqi Wang, et al. VLMEvalKit: An open-source toolkit for evaluating large
 602 multi-modality models. In *ACM MM*, 2024.

603

604 Chaoyou Fu, Peixian Chen, Yunhang Shen, Yulei Qin, Mengdan Zhang, Xu Lin, Jinrui Yang, Xiawu
 605 Zheng, Ke Li, Xing Sun, Yunsheng Wu, and Rongrong Ji. MME: A comprehensive evaluation
 606 benchmark for multimodal large language models. Preprint arXiv:2306.13394, 2024a.

607

608 Xingyu Fu, Yushi Hu, Bangzheng Li, Yu Feng, Haoyu Wang, Xudong Lin, Dan Roth, Noah A Smith,
 609 Wei-Chiu Ma, and Ranjay Krishna. BLINK: Multimodal large language models can see but not
 610 perceive. In *European Conference on Computer Vision*, pp. 148–166. Springer, 2024b.

611

612 Yunhao Gou, Kai Chen, Zhili Liu, Lanqing Hong, Hang Xu, Zhenguo Li, Dit-Yan Yeung, James T
 613 Kwok, and Yu Zhang. Eyes Closed, Safety On: Protecting multimodal LLMs via image-to-text
 614 transformation. Preprint arXiv:2403.09572, 2024.

615

616 Daya Guo, Dejian Yang, Haowei Zhang, Junxiao Song, Ruoyu Zhang, Runxin Xu, Qihao Zhu,
 617 Shirong Ma, Peiyi Wang, Xiao Bi, et al. DeepSeek-R1: Incentivizing reasoning capability in
 618 LLMs via reinforcement learning. Preprint arXiv:2501.12948, 2025.

619

620 Jiaxian Guo, Junnan Li, Dongxu Li, Anthony Meng Huat Tiong, Boyang Li, Dacheng Tao, and
 621 Steven CH Hoi. From images to textual prompts: Zero-shot VQA with frozen large language
 622 models. Preprint arXiv:2212.10846, 2022.

623

624 Yushi Hu, Hang Hua, Zhengyuan Yang, Weijia Shi, Noah A Smith, and Jiebo Luo. PromptCap:
 625 Prompt-guided task-aware image captioning. Preprint arXiv:2211.09699, 2022.

626

627 Wenzuan Huang, Bohan Jia, Zijie Zhai, Shaosheng Cao, Zheyu Ye, Fei Zhao, Zhe Xu, Yao Hu, and
 628 Shaohui Lin. Vision-R1: Incentivizing reasoning capability in multimodal large language models.
 629 Preprint arXiv:2503.06749, 2025.

630

631 Aaron Hurst, Adam Lerer, Adam P Goucher, Adam Perelman, Aditya Ramesh, Aidan Clark,
 632 AJ Ostrow, Akila Welihinda, Alan Hayes, Alec Radford, et al. GPT-4o system card. Preprint
 633 arXiv:2410.21276, 2024.

634

635 Aaron Jaech, Adam Kalai, Adam Lerer, Adam Richardson, Ahmed El-Kishky, Aiden Low, Alec
 636 Helyar, Aleksander Madry, Alex Beutel, Alex Carney, et al. Openai o1 system card. Preprint
 637 arXiv:2412.16720, 2024.

638

639 Bohao Li, Rui Wang, Guangzhi Wang, Yuying Ge, Yixiao Ge, and Ying Shan. SEED-Bench:
 640 Benchmarking multimodal llms with generative comprehension. Preprint arXiv:2307.16125, 2023.

641

642 Junnan Li, Dongxu Li, Caiming Xiong, and Steven Hoi. BLIP: Bootstrapping language-image
 643 pre-training for unified vision-language understanding and generation. In *International conference
 644 on machine learning*, pp. 12888–12900. PMLR, 2022.

645

646 Xiangyan Liu, Jinjie Ni, Zijian Wu, Chao Du, Longxu Dou, Haonan Wang, Tianyu Pang, and
 647 Michael Qizhe Shieh. NoisyRollout: Reinforcing visual reasoning with data augmentation.
 648 Preprint arXiv:2504.13055, 2025a.

649

650 Yuan Liu, Haodong Duan, Yuanhan Zhang, Bo Li, Songyang Zhang, Wangbo Zhao, Yike Yuan, Jiaqi
 651 Wang, Conghui He, Ziwei Liu, et al. MMBench: Is your multi-modal model an all-around player?
 652 In *European conference on computer vision*, pp. 216–233. Springer, 2024a.

653

654 Yuqi Liu, Tianyuan Qu, Zhisheng Zhong, Bohao Peng, Shu Liu, Bei Yu, and Jiaya Jia. Vision-
 655 reasoner: Unified visual perception and reasoning via reinforcement learning. *arXiv preprint
 656 arXiv:2505.12081*, 2025b.

648 Zhili Liu, Yunhao Gou, Kai Chen, Lanqing Hong, Jiahui Gao, Fei Mi, Yu Zhang, Zhenguo Li, Xin
 649 Jiang, Qun Liu, et al. Mixture of insightful Experts (MoTE): The synergy of thought chains and
 650 expert mixtures in self-alignment. Preprint arXiv:2405.00557, 2024b.

651

652 Zichen Liu, Changyu Chen, Wenjun Li, Penghui Qi, Tianyu Pang, Chao Du, Wee Sun Lee, and
 653 Min Lin. Understanding r1-zero-like training: A critical perspective. Preprint arXiv:2503.20783,
 654 2025c.

655

656 Pan Lu, Hritik Bansal, Tony Xia, Jiacheng Liu, Chunyuan Li, Hannaneh Hajishirzi, Hao Cheng,
 657 Kai-Wei Chang, Michel Galley, and Jianfeng Gao. MathVista: Evaluating mathematical reasoning
 658 of foundation models in visual contexts. In *ICLR*, 2024a.

659

660 Shiyin Lu, Yang Li, Qing-Guo Chen, Zhao Xu, Weihua Luo, Kaifu Zhang, and Han-Jia Ye. Ovis:
 661 Structural embedding alignment for multimodal large language model. Preprint arXiv:2405.20797,
 662 2024b.

663

664 Yiting Lu, Jiakang Yuan, Zhen Li, Shitian Zhao, Qi Qin, Xinyue Li, Le Zhuo, Licheng Wen,
 665 Dongyang Liu, Yuwen Cao, et al. OmniCaptioner: One captioner to rule them all. Preprint
 arXiv:2504.07089, 2025.

666

667 Fanqing Meng, Lingxiao Du, Zongkai Liu, Zhixiang Zhou, Quanfeng Lu, Daocheng Fu, Tiancheng
 668 Han, Botian Shi, Wenhui Wang, Junjun He, et al. MM-Eureka: Exploring the frontiers of
 669 multimodal reasoning with rule-based reinforcement learning. Preprint arXiv:2503.07365, 2025.

670

671 OpenAI. GPT-4o system card. Technical report, 2024. URL <https://arxiv.org/abs/2410.21276>.

672

673 Runqi Qiao, Qiuna Tan, Guanting Dong, Minhui Wu, Chong Sun, Xiaoshuai Song, Zhuoma GongQue,
 674 Shanglin Lei, Zhe Wei, MiaoXuan Zhang, et al. We-Math: Does your large multimodal model
 675 achieve human-like mathematical reasoning? Preprint arXiv:2407.01284, 2024.

676

677 Qwen. QVQ: To see the world with wisdom. <https://qwenlm.github.io/blog/qvq-72b-preview/>, 2024.

678

679 Alec Radford, Jong Wook Kim, Chris Hallacy, Aditya Ramesh, Gabriel Goh, Sandhini Agarwal,
 680 Girish Sastry, Amanda Askell, Pamela Mishkin, Jack Clark, et al. Learning transferable visual
 681 models from natural language supervision. In *International conference on machine learning*, pp.
 682 8748–8763. PMLR, 2021.

683

684 David Rein, Betty Li Hou, Asa Cooper Stickland, Jackson Petty, Richard Yuanzhe Pang, Julien Dirani,
 685 Julian Michael, and Samuel R Bowman. GPQA: A graduate-level google-proof q&a benchmark.
 In *COLM*, 2024.

686

687 Zhihong Shao, Peiyi Wang, Qihao Zhu, Runxin Xu, Junxiao Song, Xiao Bi, Haowei Zhang,
 688 Mingchuan Zhang, YK Li, Y Wu, et al. DeepSeekMath: Pushing the limits of mathematical
 689 reasoning in open language models. Preprint arXiv:2402.03300, 2024.

690

691 Guangming Sheng, Chi Zhang, Zilingfeng Ye, Xibin Wu, Wang Zhang, Ru Zhang, Yanghua Peng,
 692 Haibin Lin, and Chuan Wu. HybridFlow: A flexible and efficient rlhf framework. In *EuroSys*,
 2025.

693

694 Zhaochen Su, Linjie Li, Mingyang Song, Yunzhuo Hao, Zhengyuan Yang, Jun Zhang, Guanjie Chen,
 695 Jiawei Gu, Juntao Li, Xiaoye Qu, et al. Openthinkimg: Learning to think with images via visual
 696 tool reinforcement learning. *arXiv preprint arXiv:2505.08617*, 2025.

697

698 Jayant Sravan Tamarapalli, Rynaa Grover, Nilay Pande, and Sahiti Yerramilli. Countqa: How well do
 699 mllms count in the wild? *arXiv preprint arXiv:2508.06585*, 2025.

700

701 Gemma Team, Aishwarya Kamath, Johan Ferret, Shreya Pathak, Nino Vieillard, Ramona Merhej,
 Sarah Perrin, Tatiana Matejovicova, Alexandre Ramé, Morgane Rivière, et al. Gemma 3 technical
 report. Technical report, 2025a.

702 Kwai Keye Team, Biao Yang, Bin Wen, Changyi Liu, Chenglong Chu, Chengru Song, Chongling Rao,
 703 Chuan Yi, Da Li, Dunju Zang, et al. Kwai Keye-VL technical report. Preprint arXiv:2507.01949,
 704 2025b.

705 Anthony Meng Huat Tiong, Junnan Li, Boyang Li, Silvio Savarese, and Steven CH Hoi. Plug-and-
 706 play VQA: Zero-shot VQA by conjoining large pretrained models with zero training. Preprint
 707 arXiv:2210.08773, 2022.

708 Zhongwei Wan, Zhihao Dou, Che Liu, Yu Zhang, Dongfei Cui, Qinjian Zhao, Hui Shen, Jing
 709 Xiong, Yi Xin, Yifan Jiang, et al. Srp0: Enhancing multimodal llm reasoning via reflection-aware
 710 reinforcement learning. *arXiv preprint arXiv:2506.01713*, 2025.

711 Haozhe Wang, Chao Qu, Zuming Huang, Wei Chu, Fangzhen Lin, and Wenhui Chen. VL-Rethinker:
 712 Incentivizing self-reflection of vision-language models with reinforcement learning. Preprint
 713 arXiv:2504.08837, 2025a.

714 Jiayu Wang, Yifei Ming, Zhenmei Shi, Vibhav Vineet, Xin Wang, Yixuan Li, and Neel Joshi. Is a
 715 picture worth a thousand words? delving into spatial reasoning for vision language models. In *The
 716 Thirty-Eighth Annual Conference on Neural Information Processing Systems*, 2024a.

717 Ke Wang, Junting Pan, Weikang Shi, Zimu Lu, Houxing Ren, Aojun Zhou, Mingjie Zhan, and
 718 Hongsheng Li. Measuring multimodal mathematical reasoning with math-vision dataset. In
 719 *NeurIPS*, 2024b.

720 Weiyun Wang, Zhangwei Gao, Lianjie Chen, Zhe Chen, Jinguo Zhu, Xiangyu Zhao, Yangzhou Liu,
 721 Yue Cao, Shenglong Ye, Xizhou Zhu, Lewei Lu, Haodong Duan, Yu Qiao, Jifeng Dai, and Wenhui
 722 Wang. VisualPRM: An effective process reward model for multimodal reasoning. Technical report,
 723 2025b. URL <https://arxiv.org/abs/2503.10291>.

724 Weiyun Wang, Zhangwei Gao, Lianjie Chen, Zhe Chen, Jinguo Zhu, Xiangyu Zhao, Yangzhou Liu,
 725 Yue Cao, Shenglong Ye, Xizhou Zhu, et al. VisualPRM: An effective process reward model for
 726 multimodal reasoning. Preprint arXiv:2503.10291, 2025c.

727 Weiyun Wang, Zhangwei Gao, Lixin Gu, Hengjun Pu, Long Cui, Xingguang Wei, ZhaoYang Liu,
 728 Linglin Jing, Shenglong Ye, Jie Shao, et al. Internvl3. 5: Advancing open-source multimodal
 729 models in versatility, reasoning, and efficiency. Preprint arXiv:2508.18265, 2025d.

730 xAI. Grok, 2024.

731 Yijia Xiao, Edward Sun, Tianyu Liu, and Wei Wang. LogicVista: Multimodal LLM logical reasoning
 732 benchmark in visual contexts. Preprint arXiv:2407.04973, 2024.

733 An Yang, Baosong Yang, Beichen Zhang, Binyuan Hui, Bo Zheng, Bowen Yu, Chengyuan Li,
 734 Dayiheng Liu, Fei Huang, Haoran Wei, et al. Qwen2.5 technical report. Preprint arXiv:2412.15115,
 735 2024.

736 An Yang, Anfeng Li, Baosong Yang, Beichen Zhang, Binyuan Hui, Bo Zheng, Bowen Yu, Chang
 737 Gao, Chengen Huang, Chenxu Lv, et al. Qwen3 technical report. Preprint arXiv:2505.09388,
 738 2025a.

739 Yi Yang, Xiaoxuan He, Hongkun Pan, Xiyan Jiang, Yan Deng, Xingtao Yang, Haoyu Lu, Dacheng Yin,
 740 Fengyun Rao, Minfeng Zhu, et al. R1-Onevision: Advancing generalized multimodal reasoning
 741 through cross-modal formalization. Preprint arXiv:2503.10615, 2025b.

742 Kaining Ying, Fanqing Meng, Jin Wang, Zhiqian Li, Han Lin, Yue Yang, Hao Zhang, Wenbo Zhang,
 743 Yuqi Lin, Shuo Liu, et al. MMT-Bench: A comprehensive multimodal benchmark for evaluating
 744 large vision-language models towards multitask agi. Preprint arXiv:2404.16006, 2024.

745 Jiahui Yu, Zirui Wang, Vijay Vasudevan, Legg Yeung, Mojtaba Seyedhosseini, and Yonghui Wu.
 746 CoCa: Contrastive captioners are image-text foundation models. Preprint arXiv:2205.01917, 2022.

747 Qiying Yu, Zheng Zhang, Ruofei Zhu, Yufeng Yuan, Xiaochen Zuo, Yu Yue, Weinan Dai, Tiantian
 748 Fan, Gaohong Liu, Lingjun Liu, et al. DAPO: An open-source LLM reinforcement learning system
 749 at scale. Preprint arXiv:2503.14476, 2025.

756 Weihsiao Yu, Zhengyuan Yang, Linjie Li, Jianfeng Wang, Kevin Lin, Zicheng Liu, Xinchao Wang, and
757 Lijuan Wang. MM-Vet: Evaluating large multimodal models for integrated capabilities. Preprint
758 arXiv:2308.02490, 2023.

759 Xiang Yue, Yuansheng Ni, Kai Zhang, Tianyu Zheng, Ruoqi Liu, Ge Zhang, Samuel Stevens,
760 Dongfu Jiang, Weiming Ren, Yuxuan Sun, et al. MMMU: A massive multi-discipline multimodal
761 understanding and reasoning benchmark for expert agi. In *CVPR*, 2024.

762 Renrui Zhang, Dongzhi Jiang, Yichi Zhang, Haokun Lin, Ziyu Guo, Pengshuo Qiu, Aojun Zhou,
763 Pan Lu, Kai-Wei Chang, Yu Qiao, et al. MathVerse: Does your multi-modal LLM truly see the
764 diagrams in visual math problems? In *ECCV*, 2024.

765 Lianmin Zheng, Wei-Lin Chiang, Ying Sheng, Siyuan Zhuang, Zhanghao Wu, Yonghao Zhuang,
766 Zi Lin, Zhuohan Li, Dacheng Li, Eric Xing, et al. Judging LLM-as-a-judge with mt-bench and
767 chatbot arena. In *NeurIPS*, 2023.

768 Ziwei Zheng, Michael Yang, Jack Hong, Chenxiao Zhao, Guohai Xu, Le Yang, Chao Shen, and Xing
769 Yu. Deepeyes: Incentivizing" thinking with images" via reinforcement learning. *arXiv preprint*
770 arXiv:2505.14362, 2025.

771 Zetong Zhou, Dongping Chen, Zixian Ma, Zhihan Hu, Mingyang Fu, Sinan Wang, Yao Wan,
772 Zhou Zhao, and Ranjay Krishna. Reinforced visual perception with tools. *arXiv preprint*
773 arXiv:2509.01656, 2025.

774 Jinguo Zhu, Weiyun Wang, Zhe Chen, Zhaoyang Liu, Shenglong Ye, Lixin Gu, Yuchen Duan, Hao
775 Tian, Weijie Su, Jie Shao, et al. InternVL3: Exploring advanced training and test-time recipes for
776 open-source multimodal models. Preprint arXiv:2504.10479, 2025.

777 Chengke Zou, Xingang Guo, Rui Yang, Junyu Zhang, Bin Hu, and Huan Zhang. DynaMath: A
778 dynamic visual benchmark for evaluating mathematical reasoning robustness of vision language
779 models. Preprint arXiv:2411.00836, 2024.

780

781

782

783

784

785

786

787

788

789

790

791

792

793

794

795

796

797

798

799

800

801

802

803

804

805

806

807

808

809

810
 811 **Table 6: Model Configurations for each RAPID-enhanced model group in Figure 1.** “-” denotes
 812 the corresponding item (e.g., LLM reasoner, GRPO/VPO training) is not applied.

813 Size (B)	814 LLM	815 GRPO	816 VPO	817 Avg. Performance
<i>Qwen2.5-VL-3B</i>				
818 7	819 Qwen3-4B	820 ViRL39K	821 ViRL39K	822 47.3
823 11	824 Qwen3-8B	825 ViRL39K	826 ViRL39K	50.1
827 17	828 Qwen3-14B	829 ViRL39K	830 ViRL39K	831
<i>Qwen2.5-VL-7B</i>				
832 11	833 Qwen3-4B	834 ViRL39K	835 ViRL39K	836 51.0
837 15	838 Qwen3-8B	839 ViRL39K	840 ViRL39K	841 53.2
842 21	843 Qwen3-14B	844 ViRL39K	845 ViRL39K	846 53.6
<i>Qwen2.5-VL-32B</i>				
847 36	848 Qwen3-B	849 -	850 ViRL39K	851 54.6
852 40	853 Qwen3-8B	854 -	855 ViRL39K	856 55.9
857 152	858 GPT-OSS-120B	859 -	860 ViRL39K	861 57.4

829 APPENDIX

830 A LIMITATION

831 **Auto-thinking.** RAPID is specifically designed for multi-modal reasoning, and it is appealing to
 832 explore how to flexibly switch between fast and slow thinking dependent on the complexity of input
 833 queries, without human prior and prompt engineering.

834 **Domain-Specific Design.** The RAPID architecture, in its current form, is optimized for multi-modal
 835 math and science reasoning. Its extension to other domains, such as spatial reasoning (Wang et al.,
 836 2024a), would require more than re-evaluation; it would demand specific adaptations to the model
 837 itself. The experiments on general benchmarks reported in Sec. 4.1 do not test the full reasoning
 838 pipeline, as the LLM was not activated. Therefore, investigating the adaptations required to generalize
 839 RAPID remains a key open direction for future research.

840 **Adapting the LLM.** In the current implementation of RAPID, the LLM functions as a static
 841 reasoning module with its parameters kept frozen. A valuable direction for future work is to
 842 explore adapting the LLM to our perception-reasoning framework, potentially through methods like
 843 supervised fine-tuning or reinforcement learning. While this would introduce additional computational
 844 overhead for training, it remains an open empirical question whether the potential performance gains
 845 would justify the increased cost.

852 B MODEL CONFIGURATION FOR FIGURE 1

853 For each RAPID-enhanced model group (e.g., Qwen2.5-VL-3B (**RAPID**)) in Figure 1, we train the
 854 original model (e.g., Qwen2.5-VL-3B) using both the proposed VPO and GRPO objectives, where
 855 the former encourages the MLLM to generate query-relevant captions with higher quality while the
 856 later optimizes it to give better reasoning traces. The details for VPO and GRPO can be found in
 857 Sec. 4.1 and Appendix D. We then pair the trained MLLM with different LLMs under our RAPID.
 858 Table 6 shows the configuration for each RAPID-enhanced model group. Specifically, for each model
 859 in the group, we report the total model size (B), paired LLMs, data used to conduct GRPO and VPO
 860 and the average performance across 7 tasks. Note that the results for Qwen2.5-VL-32B group does
 861 not involve GRPO training because it has already undergone an RL stage before release (Bai et al.,
 862 2025). Results for other MLLMs are consistent with Table 1.

864
865
866
867
868
869
870
871
872
873
874
875
876
877
878
879
880
881
882
883
884
885
886
887
888
889
890
891
892
893
894
895
896
897
898
899
900
901
902
903
904
905
906
907
908
909
910
911
912
913
914
915
916
917Table 7: **Index of Prompt templates for RAPID.**

Component	Purpose	Notation	Prompt Template
MLLM	Holistic captions	P_{cap}	Figure 13
MLLM	Query-relevant captions	P_{qcap}	Figure 14
MLLM	Tentative response	P_{sol}	Figure 15
MLLM	Caption Penalty	-	Figure 17
LLM Reasoner	Inference	P_{reason}	Figure 12
LLM Reasoner	Reward computation	P'_{reason}	Figure 16

System Prompt:
You are a helpful assistant.

User Prompt:
In the following text, you will receive a detailed caption of an image and a relevant question. In addition, you will be provided with a tentative model response. Your goal is to answer the question using these information.

The detailed caption of the provided image: {}

A problem to be solved: {}

A tentative model response. {}

Note that the above tentative response might be inaccurate (due to calculation errors, incorrect logic/reasoning and so on), under such a case, please ignore it and give your own solutions. However, if you do not have enough evidence to show it is wrong, please output the tentative response.

Figure 12: **Prompt templates used by the reasoner LLM for inference.**

System Prompt:
You are a helpful assistant.

User Prompt:
Describe this image in detail.

Figure 13: **Prompt templates used by the MLLM to obtain the holistic captions.**

C PROMPT TEMPLATES

In Table 7, we provide an index of the prompt templates used in RAPID.

D FORMULATIONS OF GRPO

GRPO (Shao et al., 2024) is a policy optimization algorithm originally developed to enhance the reasoning capability of text-only LLMs. In our setting, the policy π_θ to optimize becomes the MLLM. For a given input pair (I, q) of image and text question from the training set p_D , the old policy generates G rollouts, *i.e.*, $o \sim \pi_{\theta_{\text{old}}}(I, P_{\text{sol}}(q))$. Denoting R_i as the reward for the i -th rollout, the normalized advantage is $\hat{A}_i = \frac{R_i - \bar{R}}{\sigma(R)}$, where $\sigma(R)$ denotes the standard deviation of rewards within the group and the baseline reward is $\bar{R} = \frac{1}{G} \sum_{i=1}^G R_i$. The objective incorporates a surrogate loss clipped within $[1 - \epsilon, 1 + \epsilon]$ ($\epsilon > 0$) and a KL-penalty $D_{\text{KL}}[\pi_\theta \| \pi_{\theta_{\text{ref}}}]$ weighted by β (not shown here)

918
919
920
921
922**System Prompt:**

You are given an image and a relevant question. Based on the query, please describe the image in detail. Do not try to answer the question.

User Prompt:

Question: {}
Please describe the image. DO NOT try to answer the question!

930

931
932
933
934
935
936
937
938
939**System Prompt:**

You are a helpful assistant.

User Prompt:

{}

946

947
948
949
950
951
952
953
954
955
956

Figure 14: **Prompt templates used by the MLLM to obtain the query-relevant captions.**

System Prompt:

You are a helpful assistant.

User Prompt:

The detailed caption of the provided image: {}

Question: {}

Please think step by step. The final answer MUST BE put in \boxed{}.

966
967
968
969
970
971

Figure 15: **Prompt templates used by the MLLM to obtain the tentative response.** The placeholder is for the question.

972
 973
 974
 975
 976
 977
 978
 979
 980
 981

System Prompt:
 You are a careful AI assistant to check whether a text contains a description of an image.

982
 983
 984

User Prompt:
 ===== Example 1 =====
 ### A text regarding an image: The image displays the logo of Huawei, featuring a red, fan-like design with the word "Huawei" written below it. This image corresponds to the question provided which involves calculating the number of components that can be inserted into a phone circuit board in one minute based on the time it takes to insert one component.
 \n\nTo solve the problem, we first need to determine how many components can be inserted in one minute. Since the production line takes \((0.01)\) seconds to insert one component, we can find out how many components can be inserted in one minute by calculating the total number of seconds in a minute and then dividing by the time it takes to insert one component.
 \n\nThere are 60 seconds in one minute. So, the number of components that can be inserted in one minute is calculated as follows:

$$\text{Number of components} = \frac{60 \text{ seconds}}{0.01 \text{ seconds/component}} = 60 \times 100 = 6000$$

 Thus, the answer is \(\boxed{6000}\).

985
 986
 987
 988
 989
 990
 991
 992
 993
 994
 995
 996
 997
 998
 999

===== Example 2 =====
 ### A text regarding an image: To solve for the length of segment \((ED)\), we first need to determine the lengths of the segments \((AC)\), \((BC)\), and \((CE)\).
 Given:
 - \((AB = 20)\)
 - \((C)\) is the midpoint of \((AB)\), so \((AC = CB = \frac{AB}{2} = \frac{20}{2} = 10)\).
 - \((D)\) is the midpoint of \((BC)\), so \((BD = DC = \frac{BC}{2} = \frac{10}{2} = 5)\).
 - \((E = \frac{2}{5}AC = \frac{2}{5} \times 10 = 4)\).
 Since \((AC = AE + CE)\) and \((AC = 10)\), we have \((AE = AC - CE = 10 - 4 = 6)\).
 Now, we need to find the length of \((ED)\). Since \((E)\) is on \((AC)\) and \((C)\) is the midpoint of \((AB)\), the coordinates of points \((A)\), \((E)\), and \((C)\) can be visualized or calculated in terms of the distances. The distance \((ED)\) can be found using the coordinates or the simpler arithmetic based on the positions:

$$ED = EC + CD = 4 + 5 = 9$$

 Thus, the length of segment \((ED)\) is \(\boxed{9}\).

1000
 1001
 1002
 1003
 1004
 1005
 1006
 1007
 1008
 1009
 1010
 1011
 1012
 1013
 1014
 1015
 1016
 1017
 1018
 1019

Does the text contains a description of the image? Please only answer yes or no:
 Yes.

Does the text contains a description of the image? Please only answer yes or no:
 No.

A text regarding an image: {}

Does the text contains a description of the image? Please only answer yes or no.

1020
 1021
 1022
 1023
 1024
 1025

Figure 17: **Prompt templates used by the MLLM for caption panely.**

1026
 1027
 1028
 1029
 1030
 1031
 1032
 1033
 1034
 1035
 1036
 1037
 1038
 1039
 1040
 1041
System Prompt:
 1042 Please act as an impartial judge and evaluate the quality of the captions provided by two multi-
 1043 modal AI assistants regarding an image and a question. You will receive an image and a question
 1044 regarding it. You should choose the caption that (i) more accurately and comprehensively reflect the
 1045 content in the image and (ii) contain more details/facts required to solve the question. (iii) contain
 1046 less visual hallucination (describing objects not shown in the image). Note that the solution to the
 1047 problem is not considered as facts or details! Note that if the caption contains any solution process,
 1048 you should ignore it (completely delete it) and only consider the remaining when conducting your
 1049 evaluation. Begin your evaluation by comparing the two captions and provide a short explanation.
 1050 Avoid any position biases and ensure that the order in which the captions were presented does not
 1051 influence your decision. Do not allow the length of the captions to influence your evaluation. Do not
 1052 favor certain names of the assistants. Be as objective as possible. After providing your explanation,
 1053 output your final verdict by strictly following this format: "[[A]]" if assistant A is better, "[[B]]" if
 1054 assistant B is better, and "[[C]]" for a tie.
 1055
User Prompt:
 1056 [User Question]
 1057 {}
 1058 [The Start of Assistant A's Caption]
 1059 {}
 1060 [The End of Assistant A's Caption]
 1061 [The Start of Assistant B's Caption]
 1062 {}
 1063 [The End of Assistant B's Caption]
 1064
 1065
 1066 Figure 18: **Prompt templates used for GPT evaluations on caption qualities.**
 1067
 1068
 1069
 1070
 1071
 1072
 1073
 1074
 1075
 1076
 1077
 1078
 1079

1080 to stabilize optimization:

$$1081 L(\theta) = \mathbb{E}_{(I, q) \sim p_{\mathcal{D}}, o \sim \pi_{\theta_{\text{old}}}(\cdot | I, P_{\text{sol}}(q))} \\ 1082 \left[\frac{1}{G} \sum_{i=1}^G \min \left(\frac{\pi_{\theta}(o_i | I, P_{\text{sol}}(q))}{\pi_{\theta_{\text{old}}}(o_i | I, P_{\text{sol}}(q))} \hat{A}_i, \text{clip} \left(\frac{\pi_{\theta}(o_i | I, P_{\text{sol}}(q))}{\pi_{\theta_{\text{old}}}(o_i | I, P_{\text{sol}}(q))}, 1 - \epsilon, 1 + \epsilon \right) \hat{A}_i \right) \right]. \\ 1083 \quad (4) \\ 1084 \\ 1085$$

1086 The reward R_i for the i -th rollout is expressed as: $R_i = r(y_{\text{gt}}, o_i) = \mathbb{1}(y_{\text{gt}} = \text{parse}(o_i))$, where y_{gt} denotes the ground-truth answer of a reasoning question and $\mathbb{1}(\cdot)$ is an indicator function that outputs 1 if the final parsed prediction matches the ground-truth and 0 otherwise.

1090 E MORE ANALYSIS

1091 E.1 ANALYSIS ON THE TRAINING COMPUTE EFFICIENCY OF RAPID

1092 RAPID’s decoupled design enables the flexible adoption of recent LLM reasoners, such as
1093 Qwen3 (Yang et al., 2025a), without retraining. This raises a critical question: *how does our efficient*
1094 *approach compare against models that require full and costly retraining of their visual-language*
1095 *alignment to integrate the latest LLMs?*

1096 To investigate this trade-off between performance and computational cost, we compare RAPID
1097 with two leading MLLMs also built on the Qwen3-8B LLM: Keye-VL (Team et al., 2025b) and
1098 InternVL3.5 (Wang et al., 2025d). Table 8 presents a comparative analysis, reporting average accuracy
1099 across seven multi-modal reasoning tasks alongside the training tokens and estimated training FLOPs
1100 (calculated as model size \times training tokens). The number of training tokens for Keye-VL-8B and
1101 InternVL3.5-8B are sourced from their respective technical reports.

1102 As can be seen, although still inferior to the end-to-end methods, RAPID with Qwen2.5-VL-7B
1103 can achieve 90.8% of Keye-VL-8B performance with $1250 \times$ less training FLOPs, and 88.2% of
1104 InternVL3.5-8B performance with $864.2 \times$ training cost reduction. Thanks to the remarkable training
1105 efficiency, we can adopt larger MLLMs such as Qwen2.5-VL-32B, we achieve comparable (92.7%)
1106 performance with InternVL3.5-8B but with $1025 \times$ less training FLOPs

1107 **Table 8: Training cost comparison.** *As we did not apply GRPO to Qwen2.5-VL-32B, it consumes
1108 less training tokens (100M) than Qwen2.5-VL-7B (550M).

Method	AVG Accuracies	# Tokens	FLOPs (Ratio)
Keye-VL-8B (Team et al., 2025b)	58.6	600B	$1500 \times$
InternVL3.5-8B (Wang et al., 2025d)	60.3	410B	$1025 \times$
Qwen2.5-VL-7B w/ RAPID (Qwen3-8B)	53.2	550M	$1.2 \times$
Qwen2.5-VL-32B w/ RAPID (Qwen3-8B)	55.9	100M*	$1 \times$

1119 E.2 ANALYSIS ON THE INFERENCE COMPUTE EFFICIENCY OF RAPID

1120 To evaluate the inference compute efficiency of RAPID, we estimate the computational cost across
1121 the seven evaluation datasets from Table 1. For each dataset, we perform inference on a sample of
1122 100 examples and approximate the compute as **model size \times number of generated tokens**. For our
1123 staged RAPID approach, the total compute is the sum from the perception and reasoning stages, with
1124 the compute for each stage calculated using its respective model size. We benchmark these results
1125 against top-performing MLLMs from Table 1. Figure 19 plots the resulting average accuracy against
1126 inference compute for both RAPID-enhanced models and their baselines.

1127 The analysis reveals two key findings:

- 1128 • **RAPID achieves a favorable trade-off between accuracy and inference compute.** This
1129 efficiency is highlighted by specific configurations that demonstrate Pareto-optimality. For
1130 instance, Qwen2.5-VL-7B w/ RAPID (R1-7B) provides a better accuracy-to-compute ratio
1131 than ReVisual-R1-7B. In another example, Qwen2.5-VL-7B w/ RAPID (Qwen3-8B)
1132 outperforms the much larger Qwen2.5-VL-72B while being more computationally efficient.

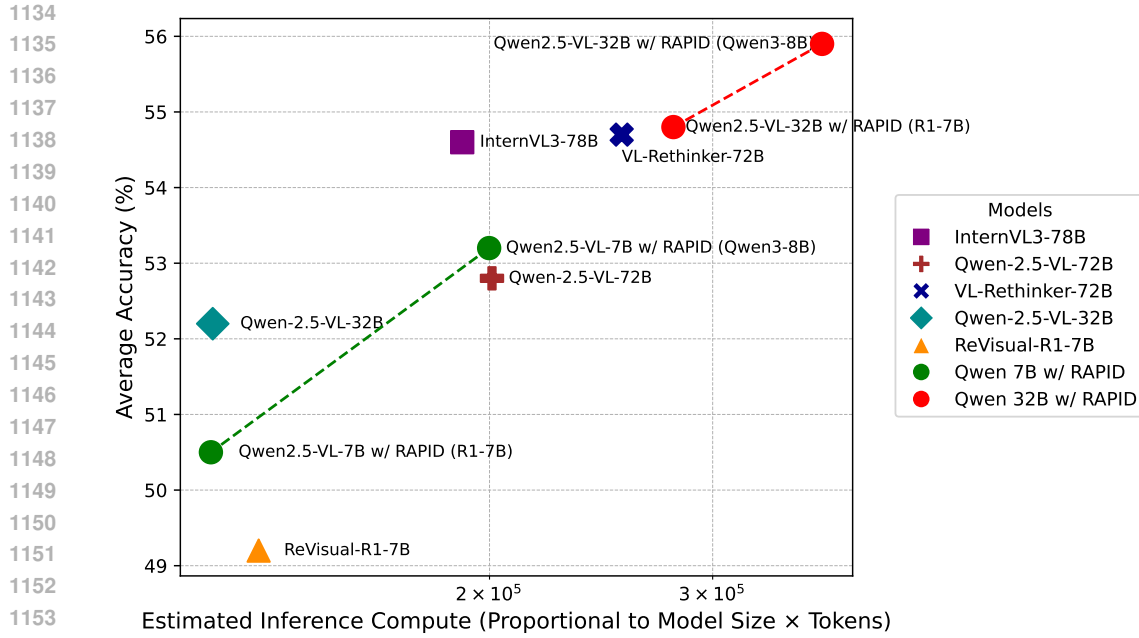


Figure 19: Inference compute versus average accuracy.

- **RAPID demonstrates strong scalability with inference compute.** The architecture is designed such that allocating more computational resources at inference—for example, by swapping in a more powerful LLM reasoner—consistently yields higher accuracy.

E.3 ANALYSIS ON THE hasCap(\cdot) CHECK AND OTHER VARIANTS

Rationale for the use of hasCap(\cdot). Our initial goal was to discourage the captioning MLLM from simply outputting a final solution instead of a descriptive caption. A key empirical finding, however, was that strictly penalizing any text containing solution-like elements was suboptimal. For many visual reasoning tasks, a descriptive caption naturally and concisely includes the answer. For instance, if asked for the time on a clock face, a good caption might be “The image shows a clock with the hands pointing to 3:15,” which contains both description and solution.

To test this, we ran an ablation study using a stricter checker that penalized the model whenever any part of the solution was detected in the output. As shown in Table 9, this variant hasSol(\cdot) performed even worse in the decoupled pipeline than no check (“None”), confirming our hypothesis that forcing a strict separation can harm performance by preventing the model from generating natural and direct descriptions.

Therefore, hasCap(\cdot) was designed as a balanced heuristic: it ensures that a caption is present but does not have to strictly forbid the co-existence of a solution.

Quantitative audit of the hasCap(\cdot) heuristic. We manually audited a random sample of 400 generations from our MLLM trained with VPO. We classified each generation into two ground-truth categories:

- **Positive Class:** The generation is a valid caption, which may or may not contain solution elements. (381 samples)
- **Negative Class:** The generation could be simply a solution or an invalid caption, such as a pure solution disguised with minimal boilerplate text (e.g., “Here is a description... [solution]”). (19 samples)

The hasCap(\cdot) prompt-based check produced the following results on this set:

Table 9: Comparisons of different checking strategies during VPO (Qwen2.5-VL-7B).

(Penalty)	Check	MathVista	MathVision	MathVerse	MMMU	WeMath	DynaMath	LogicVista	AVG
None		76.0	41.5	50.6	62.9	43.1	33.1	57.7	52.1
hasCap(\cdot)		76.1	43.7	52.2	64.7	45.4	32.7	57.7	53.2
hasSol(\cdot)		75.8	40.8	48.7	61.3	42.4	33.0	55.5	51.1

- **True Positives (TP):** 379 (Correctly identified a valid caption)
- **False Negatives (FN):** 2 (Incorrectly flagged a valid caption as invalid)
- **True Negatives (TN):** 14 (Correctly identified a gamed/invalid caption or a solution)
- **False Positives (FP):** 5 (Incorrectly identified a gamed/invalid caption or a solution as valid)

From these numbers, we can derive the following metrics for the $\text{hasCap}(\cdot)$ detector:

- **False Negative Rate:** $2/(379 + 2) = 0.525\%$
- **False Positive Rate:** $5/(5 + 14) = 26.32\%$

This audit demonstrates that the $\text{hasCap}(\cdot)$ check is highly accurate and reliable.

Analysis of Failure Modes The failure cases mostly consist of false positives (or the invalid caption ignored by the ‘ $\text{hasCap}(\cdot)$ ’ check). We found they exhibit a similar pattern (hiding pure solution in a caption-like text) as shown below:

Example of an invalid output (incorrectly identified as positive by our check):

Ok, here is a description of the image regarding the query. To find the circumference... [detailed mathematical derivation] ... Therefore, the circumference of the circle is 25.12 cm. ... This description aligns with the mathematical calculation...

Though such cases occur, they are too infrequent (5 out of 400 total samples) to impact the downstream performance.

E.4 VPO HURTS REASONING ABILITY OF THE MLLM

We note a performance decrease in the MLLM’s reasoning ability after VPO training (Table 2, rows **H** vs. **①**) and we have investigated it further.

Our analysis reveals two key findings:

- The decrease in reasoning is not permanent and can be fully recovered with a simple, subsequent fine-tuning step.
- The impact of this temporary decrease on the final, decoupled system’s performance is primarily significant for smaller models, while larger models are more robust to this effect.

Below, we elaborate on these two points.

Recovering reasoning performance with additional GRPO. To counteract this, we performed a brief, additional 100-step GRPO training stage after the VPO stage. As demonstrated in Table 10, this additional GRPO stage successfully restores the reasoning performance for both the 3B and 7B MLLMs, bringing them back to the levels seen before VPO was applied.

The impact on the decoupled framework is model-scale dependent. Interestingly, we discovered that the necessity of this recovery step depends on the scale of the MLLM backbone.

- **For the 3B Model:** We observed that the drop in reasoning after VPO did negatively impact the performance of the full decoupled pipeline. Our hypothesis is that for a smaller model, this degradation leads to lower-quality “tentative solutions” being passed to the reasoner, thereby creating a bottleneck. For this reason, we had already incorporated this additional GRPO stage for the 3B model in our original paper, as illustrated in Figure 6. This step was crucial for achieving the strong performance gains reported for the 3B model.

1242 **Table 10:** Comparisons of reasoning ability of Qwen2.5-VL-3B/7B at different stages.
1243

1244 MLLM	1245 Math Vista	1246 Math Vision	1247 Math Verse	1248 MMMU	1249 We Math	1250 Dyna Math	1251 Logic Vista	1252 AVG
3B (GRPO)	69.1	26.9	38.2	56.9	34.0	20.0	42.5	41.1
3B (GRPO+VPO)	68.8	26.9	39.8	49.4	33.0	21.6	46.3	40.8
3B (GRPO+VPO+GPRO)	69.1	26.9	39.8	55.1	33.3	20.5	44.0	41.2
7B (GRPO)	74.2	29.7	44.8	55.9	41.0	27.7	48.1	45.9
7B (GRPO+VPO)	75.0	29.8	42.0	55.8	40.8	23.0	46.3	44.7
7B (GRPO+VPO+GPRO)	74.5	29.8	44.3	55.9	40.7	28.5	48.1	46.0

1253 **Table 11:** Decoupling results of Qwen2.5-VL-7B at different stages.
1254

1252 MLLM	1253 Math Vista	1254 Math Vision	1255 Math Verse	1256 MMMU	1257 We Math	1258 Dyna Math	1259 Logic Vista	1260 AVG
7B (GRPO+VPO) + Qwen3-8B	76.1	43.7	52.2	64.7	45.4	32.7	57.7	53.2
7B (GRPO+VPO+GPRO)+ Qwen3-8B	76.5	43.6	52.4	63.9	44.8	33.3	57.3	53.1

1261 • **For the 7B Model:** Although applying the extra GRPO stage to the 7B model restored
1262 its own reasoning ability (Table 10), it yielded no significant improvement for the final
1263 decoupled system (Table 11). Therefore, to maintain the methodological simplicity of
1264 RAPID, we omitted this non-essential step for the 7B model in our paper.

1265 E.5 ANALYSIS ON THE EFFECT OF CAPTION LENGTH

1266 In our original analysis (Figure 9 in Section 4.2), the final performance correlates with both the choice
1267 of LLM for reward computation and the length of the generated captions. This raises the question of
1268 whether caption length is the primary causal factor for the performance difference.

1269 To isolate the effect of caption length, we conducted a controlled experiment. Our goal was to
1270 decouple the reward model’s identity from the resulting caption length. We started with the setup
1271 that uses, Qwen3-8B, the stronger reasoner, to compute the VPO reward, which normally results
1272 in shorter captions (average 153 tokens) and worse performance. We then introduced an explicit
1273 length-controlled reward to encourage the perception model (Qwen2.5-VL-7B) to generate longer
1274 captions, matching the average length produced when using R1-7B for rewards (approx. 654 tokens).

1275 To achieve this, we added a length penalty term to the reward function, as formulated in Aggarwal &
1276 Welleck (2025): $r_{len}(y, n_{target}) = -\alpha|n_{target} - n_y|$. Here, n_{target} was set to 650, n_y is the token count
1277 of the generated caption y , and the weight α was set to 0.0003 as per Aggarwal & Welleck (2025).

1278 This approach successfully controlled the output length; the average caption length for the model
1279 trained with Qwen3-8B rewards increased from around 153 to around 627 tokens, as intended. We
1280 then evaluated this MLLM on our benchmark suite, with the results presented in Table 12. The model
1281 trained with length-controlled rewards showed a minor performance improvement over the baseline
1282 model trained with standard Qwen3-8B rewards. However, its performance still significantly lags
1283 behind the model trained with R1-7B as the reward source.

1284 This outcome leads to a clear conclusion. Forcing the MLLM to generate longer text does not
1285 guarantee more comprehensive or useful descriptions. Instead, the model may produce verbose but
1286 less informative content to satisfy the length constraint. This result allows us to eliminate caption
1287 length as a confounding variable, confirming that the performance gap is attributable to the reasoning
1288 ability of the LLM that generates the reward signal.

1289 E.6 ADAPTING THE LLM TO REASON OVER CAPTIONS VIA FINE-TUNING

1290 We conducted an experiment where we fine-tuned the LLM reasoner (Qwen3-8B) in a separate
1291 stage after VPO on the ViRL-39K dataset. The training data for the LLM consisted of the captions
1292 generated by our VPO-trained MLLM (Qwen2.5-VL-7B). We then applied the same GRPO objective
1293 (with a group-size of 4) to optimize the reasoner.

1294 However, the experiment did not yield significant improvements. During training, we observed
1295 that the reward signal was highly unstable, fluctuating without a consistent upward trend. The final
1296 evaluation results, as shown in Table 13, confirmed this observation, revealing only marginal gains.

1296 Table 12: Correlation between the choices of LLM, the length of the captions and final performance.
1297

1298 LLM	1299 Length	1300 MathVista	1301 MathVision	1302 MathVerse	1303 MMMU	1304 WeMath	1305 DynaMath	1306 LogicVista	1307 AVG
R1-7B	653.7	76.1	43.7	52.2	64.7	45.4	32.7	57.7	53.2
Qwen3-8B	153.1	75.8	40.8	48.7	61.3	42.4	33.0	55.5	51.1
Qwen3-8B (length-controlled)	627.1	75.8	40.8	48.7	61.3	42.4	33.0	55.5	51.1

1302 Table 13: Adapting the LLM to reason over captions via GPRO training.
1303

1304 Models	1305 MathVista	1306 MathVision	1307 MathVerse	1308 MMMU	1309 WeMath	1310 DynaMath	1311 LogicVista	1312 AVG
RAPID	76.1	43.7	52.2	64.7	45.4	32.7	57.7	53.2
RAPID (LLM trained)	77.1	43.4	53.2	63.3	45.1	33.3	57.5	53.3

1309 Our hypothesis is that a powerful, pre-trained LLM like Qwen3-8B already possesses robust reasoning
1310 capabilities that generalize effectively to understanding captions. Consequently, further fine-tuning
1311 provides diminishing returns, especially when the base model’s reasoning is already strong.

1312 E.7 USING THE SAME MLLM FOR REASONING

1314 We conducted a new experiment using the same trained MLLM, Qwen2.5-VL-7B (GRPO+VPO),
1315 for both the perception (captioning) and reasoning stages of our decoupled pipeline. Note that for
1316 this case, it is not actually a “decoupling” result as the image is visible to the reasoner. In Table 14,
1317 we compare this “decouple with self” approach against the standard end-to-end usage of the same
1318 MLLM, where it processes the image and question simultaneously.

1320 As the table shows, applying our decoupled pipeline even with the same model for both stages
1321 yields a tangible performance improvement (46.1% vs. 44.7% average). This demonstrates that the
1322 structured two-stage process of first externalizing perception into text and then performing reasoning
1323 is beneficial in itself. However, it still lags behind when using Qwen3-8B, the default setting of our
1324 main paper, as the reasoner, which could be possibly attributed to their gap in reasoning capacity.

1325 F MORE EXPERIMENTAL DETAILS

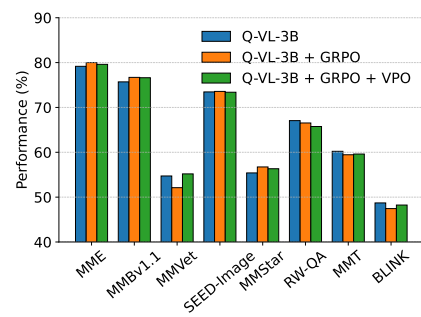
1326 F.1 EVALUATION ON GENERAL BENCHMARKS

1329 We select MME (Fu et al., 2024a), MMBench-v1.1 (Liu
1330 et al., 2024a), MM-Vet (Yu et al., 2023), SEED-
1331 Image¹⁰ (Li et al., 2023), MMstar (Chen et al., 2024),
1332 RealWorld-QA (RW-QA) (xAI, 2024), MMT-Bench
1333 (MMT) (Ying et al., 2024), and BLINK (Fu et al., 2024b)
1334 to assess foundational vision-language capabilities, which
1335 cover tasks such as object recognition, text recognition
1336 (OCR), spatial awareness and so on. Figure 20 presents the
1337 results for Qwen2.5-VL-3B. Similar to the observations
1338 for the 7B model (Figure 5), the VPO/GRPO-optimized
1339 model performs comparably to the original MLLM (Note
1340 we do not report results with Qwen2.5-VL-32B/72B as
1341 they show the same observations). This confirms that
1342 RAPID preserves general-purpose abilities across different
1343 model scales.

1344 F.2 ABLATION STUDY ON QWEN2.5-VL-3B

1346 In this section, we extend our ablation study to the smaller Qwen2.5-VL-3B model, with results
1347 presented in Table 15. While the results are largely consistent with those from its 7B counterpart
1348 (Table 2), a critical difference emerges. The 3B model necessitates an additional GRPO stage (F)

1349 ¹⁰We evaluated on the “Image” split.



1350 Figure 20: General benchmark Results.
(Qwen-2.5-VL-3B)

1350
1351 Table 14: Performance comparison between decoupling (the same MLLM performing both captioning
1352 and reasoning) and an end-to-end MLLM. Qwen2.5-VL-7B (GRPO+VPO) is adopted.
1353
1354

LLM	MathVista	MathVision	MathVerse	MMMU	WeMath	DynaMath	LogicVista	AVG
Decouple	73.7	30.0	44.0	57.3	41.0	27.3	49.2	46.1
End-to-end	75.0	29.8	42.0	55.8	40.8	23.0	46.3	44.7

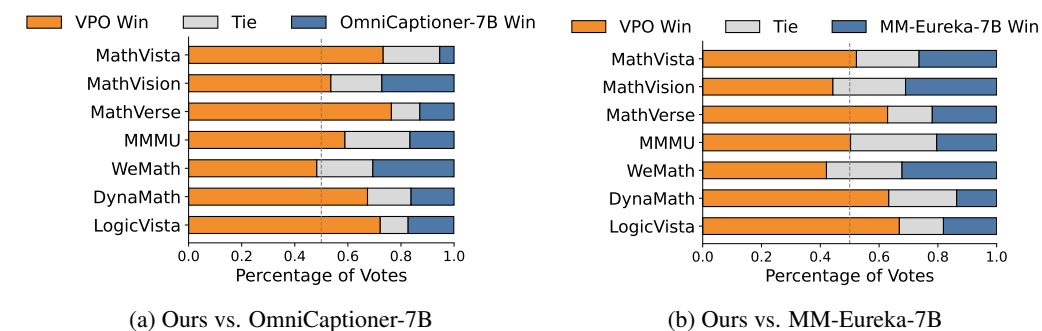
1355
1356
1357 Table 15: **Ablation study of different components of RAPID** (with Qwen2.5-VL-3B). VPO[†]: VPO
1358 without the caption penalty; [‡]: using cap+sol for reasoning-perception decoupling. *: After VPO,
1359 we additionally conduct GRPO to recover its reasoning ability.
1360

	Decouple	GRPO	VPO [†]	Cap. penalty	Math Vista	Math Vision	Math Verse	MMMU	We Math	Dyna Math	Logic Vista	AVG
Ⓐ					64.5	21.9	28.8	50.1	24.2	13.4	39.6	34.6
Ⓑ	✓				65.5	39.1	31.9	59.0	31.1	24.8	48.3	42.8
Ⓒ	✓	✓			68.5	40.0	39.2	61.0	35.1	26.9	51.7	46.1
Ⓓ	✓	✓	✓		68.5	39.4	43.4	59.9	37.4	27.9	<u>55.3</u>	47.4
Ⓔ	✓	✓	✓	✓	69.0	39.7	44.3	60.9	38.6	27.3	<u>55.3</u>	47.9
Ⓕ	✓	✓*	✓	✓	69.6	40.8	48.6	<u>60.9</u>	39.1	29.3	56.4	49.2
Ⓖ	✓ [‡]	✓	✓	✓	67.0	40.9	44.3	58.0	33.2	28.9	54.4	46.7
Ⓗ	✓		✓	✓	68.8	41.0	43.8	59.8	34.8	28.7	54.4	47.3
Ⓘ		✓			<u>69.1</u>	26.9	38.2	56.9	34.0	20.0	42.5	41.1
Ⓣ		✓	✓	✓	68.8	26.9	39.8	49.4	33.0	21.6	46.3	40.8

1371 following VPO to restore its reasoning capabilities¹¹, which in turn yields considerable accuracy
1372 gains. We attribute this requirement to the limited capacity of the 3B model, where optimizing for the
1373 VPO task appears to degrade its inherent reasoning performance—a trade-off that is less pronounced
1374 in the larger 7B model.
1375

1376 F.3 DETAILS FOR PAIRWISE COMPARISONS

1377
1378 **Extended comparisons with OmniCaptioner-7B and MM-Eureka-7B.** Following the setting in
1379 Sec. 4.4, we conducted a head-to-head comparison of our model, Qwen2.5-VL-7B (GRPO+VPO),
1380 against two strong baselines: OmniCaptioner-7B (an MLLM enhanced for holistic captioning) and
1381 MM-Eureka-7B (an MLLM specially optimized for reasoning)
1382



1393 Figure 21: Pairwise comparisons on caption quality among ours and OmniCaptioner-7B/MM-Eureka.
1394

1395
1396 The win/tie/lose rates for Qwen2.5-VL-7B (GRPO+VPO) are reported in Figure 21 where we observe
1397 the following:
1398

- **RAPID vs. OmniCaptioner-7B:** Our model’s advantage stems from its focus on generating query-relevant captions, in contrast to OmniCaptioner’s holistic captions. Our model also benefits from a more advanced base model (Qwen2.5-VL-7B vs. Qwen2-VL-7B).

1399
1400
1401
1402
1403 ¹¹We hypothesize that VPO degrades the quality of the intermediate reasoning steps passed to the LLM, an effect not always visible in the final accuracy.

1404
1405
1406

- **RAPID vs. MM-Eureka-7B:** Our model performs better because VPO directly optimizes
for captioning quality, whereas MM-Eureka-7B is optimized for end-to-end reasoning.

1407
1408
1409
1410
1411
1412
1413
1414

This validates that VPO significantly enhances the MLLM’s ability to generate high-quality, task-relevant descriptions, outperforming MLLMs specialized for either holistic captioning or reasoning.

1415
1416
1417
1418
1419
1420
1421
1422
1423

Prompt for GPT evaluations. We provide the prompt for GPT evaluations on the quality of the caption in Figure 18. Consistent with the details in Sec. 4.4, this instructs the GPT to (1) choose captions that include more comprehensive and accurate details required to answer the question and (2) exclude any solving process in the captions.

1424
1425
1426
1427
1428
1429
1430
1431
1432
1433
1434
1435
1436
1437
1438
1439
1440
1441
1442
1443
1444
1445
1446
1447
1448
1449
1450
1451
1452
1453
1454
1455
1456
1457

Human evaluations. We present the details of the human evaluation conducted for the pairwise comparison experiment. For this, 100 questions are randomly sampled from the testmini set of MathVista, and captions are generated using Qwen2.5-VL-3B, trained with and without VPO. A total of 4 trained human annotators are recruited, with each annotator comparing all the captions pairs to determine a winner or a tie. For each caption pair, we aggregate the results from different annotators by taking the majority of the decisions. Specifically, there are 4 annotators and only 3 decisions (win, tie and lose), so there is at least one decision that occurs twice. We compute the **inter-annotator consistency** following Zheng et al. (2023) by calculating the ratio of identical decision pairs out of all possible decision pairs and average them across all samples.

In Table 16, we report the win/tie/lose ratio (*i.e.*, “win” means captions generated by MLLMs with VPO is better) and an additional measure of **GPT-human consistency**, calculated by the agreement rate between GPT-4o and human judgments. As can be seen, Qwen2.5-VL-3B trained with VPO demonstrates superior caption quality under human evaluation. This aligns with the result in Figure 11, which is further supported by the high consistency of 87%. This supports the rationale of using GPT-4o as a judge for evaluating caption quality.

Table 16: **Human evaluation on pairwise comparison of the caption quality.**

Win	Tie	Lose	GPT-human consistency	Inter-annotator consistency
62%	32%	6%	87%	85%

F.4 EXTENDING DECOUPLING TO OTHER MLLMs.

We apply the decoupling pipeline alone to more MLLMs (*i.e.*, InternVL3-8B, VL-Rethinker-7B and MM-Eureka-7B) with different LLMs (*i.e.*, Qwen3-8B and GPT-OSS-120B) and report the results in Table 17.

F.5 TRAINING DYNAMICS OF VPO

We show the average reward and caption lengths over training in Figures 22 and 23. We observe that:

- **Rewards increased as training progresses.** This confirms the effectiveness of VPO as it allows the MLLM to generate captions that lead to higher reasoning accuracy.
- **Caption lengths grow as training progresses.** An explanation for this phenomenon is that the MLLM learns to generate more comprehensive captions during training, which is reflected by longer lengths. This is also confirmed in the Appendix I, where we visualize the captions.

F.6 TRAINING DYNAMICS OF GRPO

We visualize the training dynamics of GRPO in Figure 24. For 3B and 7B MLLMs, the rewards fluctuate and eventually drop after an initial convergence. In contrast, the 72B model exhibits a more stable convergence. In both cases, subsequent VPO stage continues to improve the performance under the perception-reasoning pipelines.

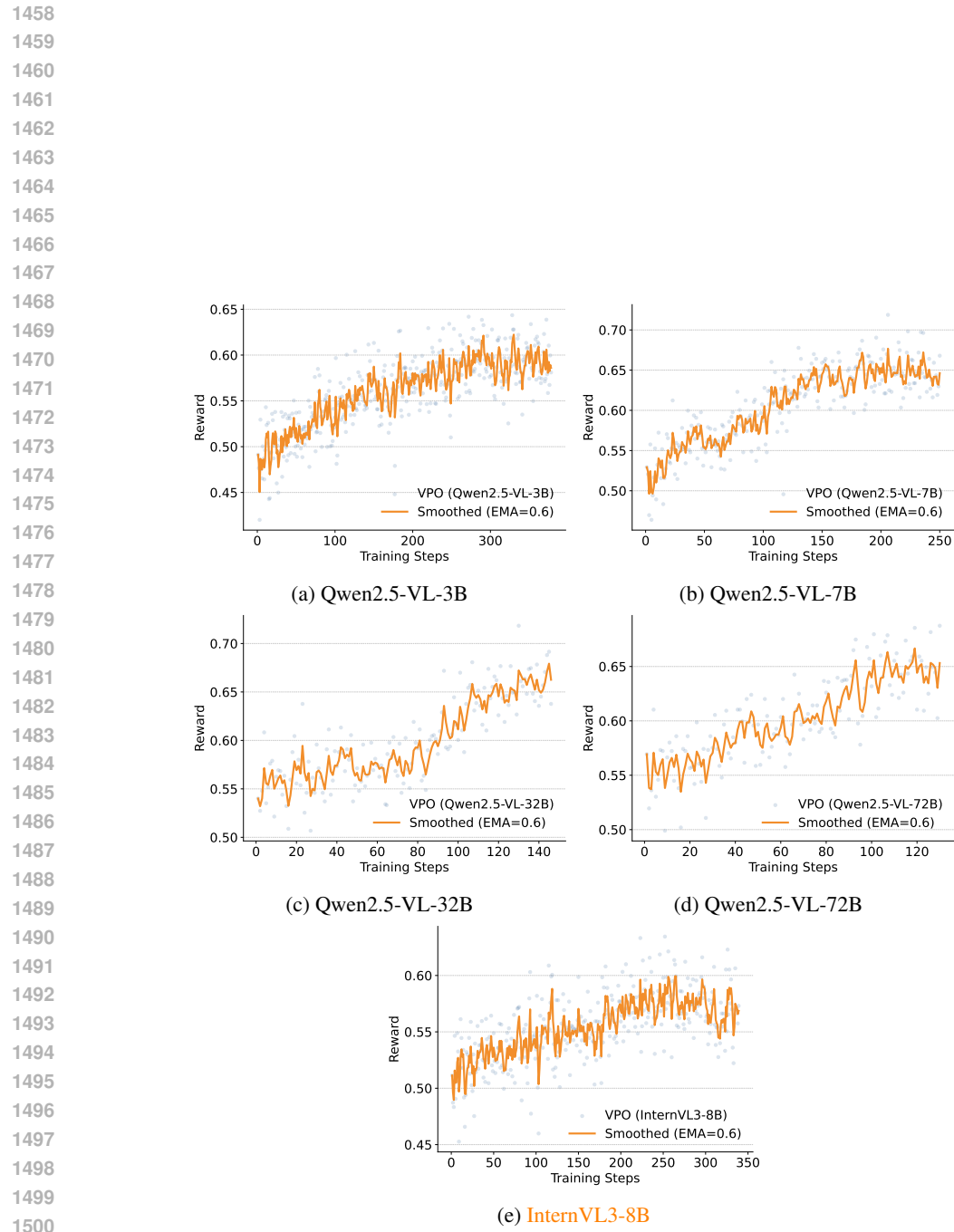


Figure 22: Rewards over training steps for VPO.

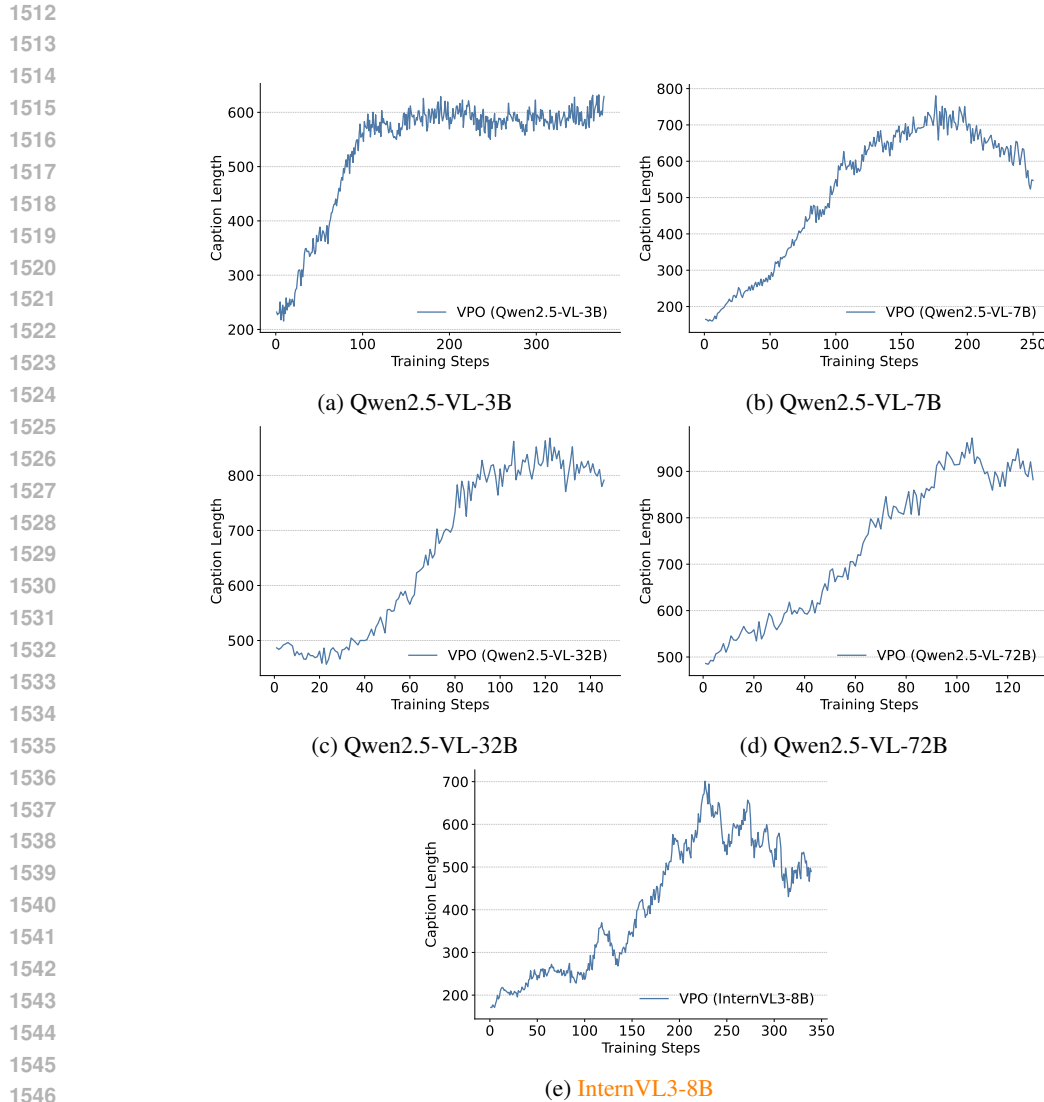


Figure 23: Caption length over training steps for VPO.

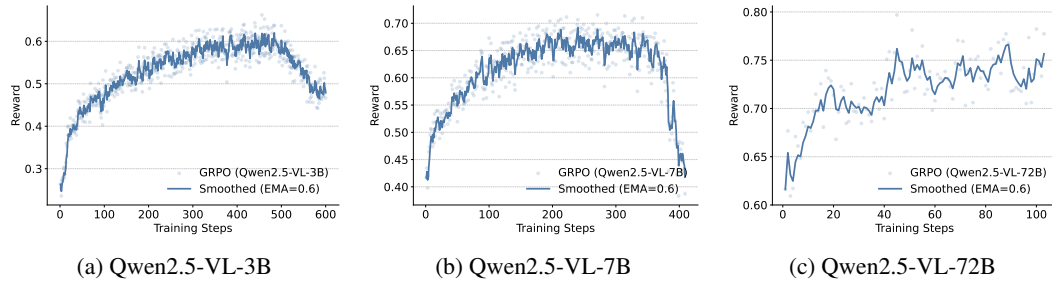


Figure 24: Rewards over training steps for GRPO.

1566 Table 17: **Decoupling (using Qwen3-8B and GPT-OSS-120B) performance of different MLLMs.**
 1567 The best results are **bold**.

Model	MathVista	MathVision	MathVerse	MMMU	WeMath	DynaMath	LogicVista	AVG
InternVL3-8B	73.6	29.3	39.8	62.7	37.1	25.5	44.1	44.6
w/ Qwen3-8B	71.3	42.4	39.3	64.4	38.8	29.1	50.1	47.9
w/ GPT-OSS-120B	70.6	47.1	41.2	68.1	41.0	29.1	51.0	49.7
VL-Rethinker-7B	74.9	30.0	47.5	56.9	37.3	21.4	43.6	44.5
w/ Qwen3-8B	72.8	43.0	51.9	59.7	41.1	30.9	52.3	50.2
w/ GPT-OSS-120B	72.8	47.8	50.0	68.1	46.3	30.7	55.0	53.0
MM-Eureka-7B	73.0	27.9	46.1	54.9	34.7	22.6	48.3	43.9
w/ Qwen3-8B	72.2	42.1	47.7	61.4	35.9	28.9	51.2	48.5
w/ GPT-OSS-120B	70.5	47.5	51.8	68.2	43.9	33.5	50.8	52.3

G MORE DISCUSSIONS

G.1 ADVANTAGES OF RAPID OVER UNIFIED ARCHITECTURE

We are aware that RAPID is a modular framework rather than a unified architecture that is adopted by most existing MLLMs. Our perspective is that RAPID are not to replace these unified systems, but rather to serve a dual, complementary role. Specifically, it could serve as a data engine to build future powerful unified models. However, under limited budget, it could be a pragmatic and economic solution to address capacity gap of unified models.

RAPID as a Data Engine for Future Unified Models. We agree that a powerful, unified MLLM is the ultimate goal. However, training such models is hampered by the scarcity of high-quality, multi-modal reasoning data. Our modular framework directly addresses this bottleneck. The RAPID pipeline can generate vast amounts of complex reasoning trajectories. This high-quality, model-generated data can then be used to train and significantly improve a future unified MLLM, a technique proven effective in prior work (Yang et al., 2025b; Huang et al., 2025).

RAPID-like Methods Bridge Current Ability Gap. At present, general-purpose MLLMs still lag behind specialized models in critical perception tasks like object counting (Tamarapalli et al., 2025), fine-grained OCR (Chen et al., 2025b), depth estimation (Fu et al., 2024b) and semantic segmentation (Anonymous, 2025). However, expert-agent-based systems could pragmatically bridge this gap by integrating these “expert” models (Zhou et al., 2025; Su et al., 2025; Liu et al., 2025b). This allows the system to leverage SoTA performance on these sub-tasks immediately, achieving higher overall accuracy.

RAPID as an Economic Solution with Limited Compute. While a unified architecture is a compelling goal, RAPID is a more pragmatic solution under restricted training budgets. It circumvents the prohibitive cost of training a unified model on massive data. For example, RAPID could enjoy the advanced reasoning ability of new LLMs without training a new MLLM from scratch.

H USE OF LARGE LANGUAGE MODELS (LLMs)

In this paper, the role of Large Language Models (LLMs) was confined to a minor, supporting capacity for polishing the writing. They were not involved in the core research process, such as ideation or analysis.

I CASE STUDY

Caption qualities. We conduct a case study on the generated query-relevant captions. Specifically, for a multi-modal reasoning question and image, we investigate the quality of the generated captions. For MLLMs, we consider Qwen2.5-VL series (3B/32B) both with and without VPO. We visualize the question, image and captions in Tables 18- 24 for Qwen2.5-VL-3B and Tables 25- 29 for Qwen2.5-VL-32B.

1620
1621

Comparing the captions generated by MLLMs with and without VPO, we discover the following:

1622
1623
1624
1625

- **VPO leads to more visual details.** We highlight these visual details in red in the table. Notably, these details are important clues required to correctly solve the question. This shows that VPO is effective in improving the quality (especially comprehensiveness) of the query-relevant captions.
- **VPO leads to captions with more organized and hierarchical structures.** For example, in Table 23, the MLLM with VPO describes the images at three levels, *i.e.*, Tropic level, Terrestrial food chain and aquatic food chain. This allows the reasoner to quickly locate important information in the captions. However, the original MLLM uses a sequence of sentences that are less clear.
- **Large-sized MLLMs generate more comprehensive captions.** We found the captions generated by Qwen2.5-VL-32B are significantly longer than those generated by the 3B model. This is because larger MLLMs have better reasoning abilities that allow it to describe the image from multiple perspectives and in a more logically coherent way. This leads to longer captions.

1636

Reasoning accuracies. In Table 30, we provide a complete comparison of captions (generated by Qwen2.5-VL-3B with and without VPO) and the resulting reasoning results (produced by R1-7B). Similarly to the case study on caption quality, MLLMs trained with VPO generate captions that capture more details. This is critical to the correctness of the reasoning process. As can be seen, the reasoner that receives captions with VPO arrives at the correct answer after several rounds of thinking and reflection. *However, the reasoner that accepts the under-optimized caption experiences multiple contradictions and confusion (highlighted in brown), which leads to responses that exceeds the maximum context length and finally fails this problem.*

1644

1645
1646

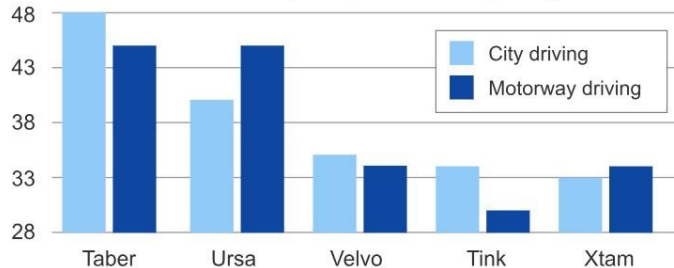
Table 18: **Case Study with Qwen2.5-VL-3B.** Additional visual details that are relevant to the question but are only generated by MLLMs with VPO are highlighted in red.

1647

1648

Image:

Fuel Consumption (miles to the gallon)



1649

1650

1651

1652

1653

1654

1655

1656

1657

1658

1659

1660

1661

1662

1663

1664

1665

1666

1667

1668

1669

1670

1671

1672

1673

Car	Max. Speed (mph)	Cost to Purchase (£)
Taber	65	12,500
Ursa	60	15,250
Velvo	125	37,500
Tink	95	55,250
Xtam	110	62,500

Question:

If a driver travels an average of 4,250 miles per month driving only along motorways in an Xtam car, what is the predicted annual consumption of fuel (in gallons)? Select from A, B, C, D and E.
 (A) Cannot say (B) 1,500 (C) 125 (D) 150 (E) 1,250

Query-relevant Captions (Qwen2.5-VL-3B w/ VPO):

1674 The image is a bar graph titled “Fuel Consumption (miles to the gallon)” that compares the fuel
 1675 efficiency of five different cars, labeled as Taber, Ursu, Velvo, Tink, and Xtam. The graph is divided
 1676 into two categories: “City driving” and “Motorway driving.”
 1677 For each car, there are two bars:
 1678 - The light blue bar represents fuel consumption for city driving.
 1679 - The dark blue bar represents fuel consumption for motorway driving.
 1680 **The data for each car is as follows:**
 1681 **- Taber:**
 1682 City driving: 48 miles per gallon
 1683 Motorway driving: 43 miles per gallon
 1684 **- Ursu:**
 1685 City driving: 39 miles per gallon
 1686 Motorway driving: 43 miles per gallon
 1687 **- Velvo:**
 1688 City driving: 35 miles per gallon
 1689 Motorway driving: 33 miles per gallon
 1690 **- Tink:**
 1691 City driving: 33 miles per gallon
 1692 Motorway driving: 28 miles per gallon
 1693 **- Xtam:**
 1694 City driving: 33 miles per gallon
 1695 Motorway driving: 33 miles per gallon
 1696 Below the bar graph, there is a table that provides additional information about each car:
 1697 - **Max. Speed (mph):** Taber (65), Ursu (60), Velvo (125), Tink (95), Xtam (110)
 1698 - **Cost to Purchase (£):** Taber (12,500), Ursu (15,250), Velvo (37,500), Tink (55,250), Xtam (62,500)
 1699 The image does not contain any information related to the question about fuel consumption for a
 1700 specific car model.

1701 **Query-relevant Captions (Qwen2.5-VL-3B):**
 1702 The image is a bar graph titled “Fuel Consumption (miles to the gallon)” that compares the fuel
 1703 efficiency of five different cars, Taber, Ursu, Velvo, Tink, and Xtam, under two driving conditions:
 1704 city driving and motorway driving. The graph uses two colors to differentiate between these
 1705 conditions: light blue for city driving and dark blue for motorway driving.

1706 Below the graph, there is a table that provides additional information about each car, including:
 1707 - **Max. Speed (mph):** The maximum speed each car can achieve.
 1708 - **Cost to Purchase (£):** The price of each car in pounds.

1709 The table entries are as follows:
 1710 **- Taber:**
 1711 Max. Speed: 65 mph
 1712 Cost to Purchase: £12,500
 1713 **- Ursu:**
 1714 Max. Speed: 60 mph
 1715 Cost to Purchase: £15,250
 1716 **- Velvo:**
 1717 Max. Speed: 125 mph
 1718 Cost to Purchase: £37,500
 1719 **- Tink:**
 1720 Max. Speed: 95 mph
 1721 Cost to Purchase: £55,250
 1722 **- Xtam:**
 1723 Max. Speed: 110 mph
 1724 Cost to Purchase: £62,500

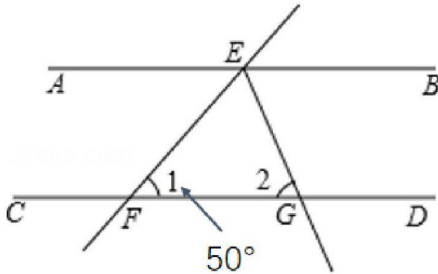
1725 The graph shows that the Taber and Ursu cars have higher fuel efficiency in city driving compared to
 1726 motorway driving, while the Velvo, Tink, and Xtam cars have higher fuel efficiency in motorway
 1727 driving compared to city driving.

1728

1728
1729 Table 19: **Case Study with Qwen2.5-VL-3B.** Additional visual details that are relevant to the
1730 question but are only generated by MLLMs with **VPO** are highlighted in red.
1731

1732 **Image:**

1733 As shown in the figure, AB parallel CD, EG bisects angle BEF,
1734 then angle 2 is equal to ()
1735 Choices: A:50° B:60° C:65° D:90°



1744 **Question:**

1745 According to the question shown in the image, please directly answer the question and provide the
1746 correct option letter, e.g., A, B, C, D.
1747

1748 **Query-relevant Captions (Qwen2.5-VL-3B w/ VPO):**

1749 The image is a geometric diagram with the following elements:

- 1750 - Two parallel lines labeled *AB* and *CD*.
- 1751 - A line segment *EF*.
- 1752 - A point *G* where line segment *EG* intersects line segment *CD*.
- 1753 - An angle labeled 50° at point *F*.
- 1754 - An angle labeled *2* at point *G*.
- 1755 - A question asking about the measure of angle *2*, with choices:
A: 50°
B: 60°
C: 65°
D: 90°

1759 The diagram shows a triangle $\triangle EFG$ with angle 1 at point *F* and angle 2 at point *G*.

1760 The angle at point *F* is given as 50° .

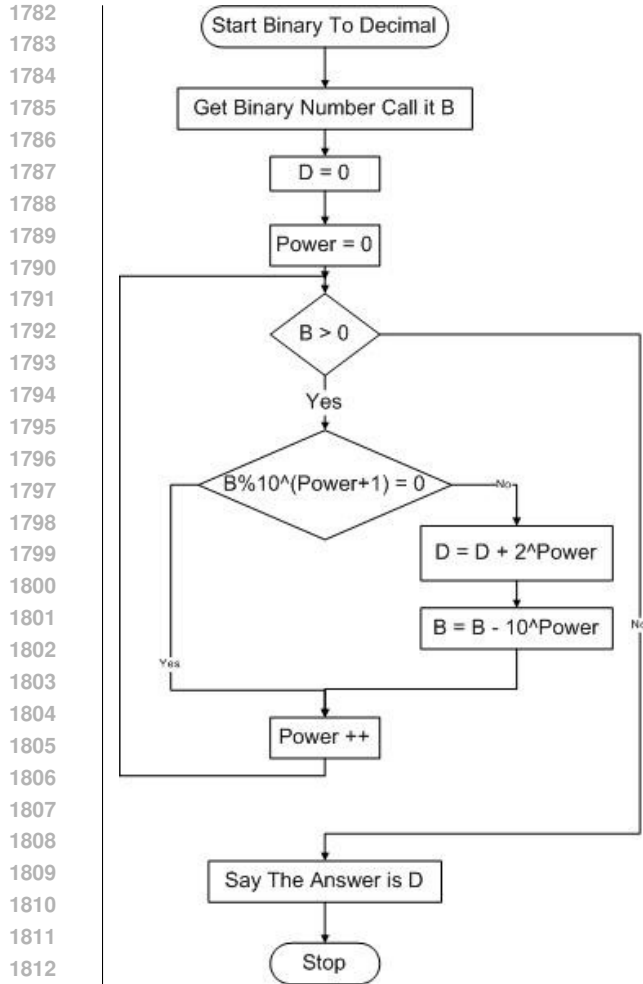
1761 The question asks for the measure of angle 2, given that $AB \parallel CD$ and *EG* bisects angle $\angle BEF$.

1762 **Query-relevant Captions (Qwen2.5-VL-3B):**

1763 The image shows a geometric figure with lines *AB* and *CD* parallel to each other. Line *EG* bisects
1764 angle *BEF*. Angle 1 is marked as 50 degrees.

1767 Table 20: **Case Study with Qwen2.5-VL-3B.** Additional visual details that are relevant to the
1768 question but are only generated by MLLMs with **VPO** are highlighted in red.
1769

1770 **Image:**

**Question:**

Input binary number $B = 11000$, find the corresponding decimal value by the algorithm shown in image.

Query-relevant Captions (Qwen2.5-VL-3B w/ VPO):

The image is a flowchart titled "Start Binary To Decimal." It outlines a process to convert a binary number to its decimal equivalent. The flowchart starts with the instruction "Get Binary Number Call it B," which is followed by initializing variables D and Power to 0. The flowchart then checks if B is greater than 0. If B is greater than 0, it checks if B modulo 10 raised to the power of (Power + 1) is equal to 0. If this condition is false, it updates D by adding 2 raised to the power of Power, and then updates B by subtracting 10 raised to the power of Power. If the condition is true, it increments Power. This process continues until B is no longer greater than 0. Finally, it states "Say The Answer is D" and "Stop."

The image does not contain any visual elements or additional information beyond the flowchart itself.

Query-relevant Captions (Qwen2.5-VL-3B):

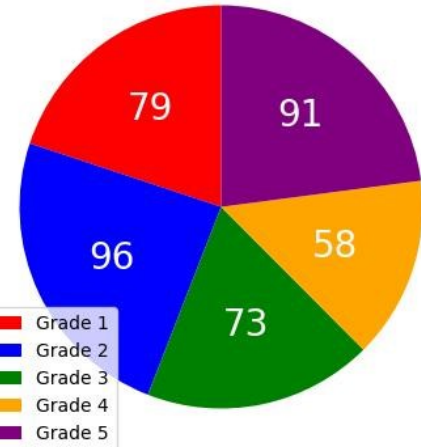
Start Binary To Decimal
 Get Binary Number Call it B
 $D = 0$
 $Power = 0$
 $B > 0$
 $B \% 10^{(Power + 1)} = 0$
 $D = D + 2^{Power}$
 $B = B - 10^{Power}$

1836
 1837 Yes
 1838 Power ++
 1839

1840 Table 21: **Case Study with Qwen2.5-VL-3B.** Additional visual details that are relevant to the
 1841 question but are only generated by MLLMs with **VPO** are highlighted in red.
 1842

1843 **Image:**

1844 Number of Students in Each Grade



1863 **Question:**

1864 The pie chart below represents the number of each grade at a United States elementary school. What
 1865 is the percentage of Grade 2? The answer should be a percentage between 0 and 100.

1866 **Query-relevant Captions (Qwen2.5-VL-3B w/ VPO):**

1867 The image is a pie chart titled "Number of Students in Each Grade." The chart is divided into five
 1868 segments, each representing a different grade level and the number of students in that grade. The
 1869 grades and their corresponding numbers are as follows:

- 1870 - Grade 1: 79 students
- 1871 - Grade 2: 96 students
- 1872 - Grade 3: 73 students
- 1873 - Grade 4: 58 students
- 1874 - Grade 5: 91 students

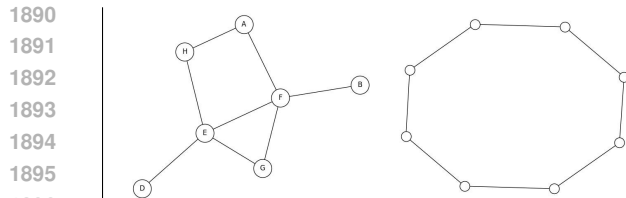
1875 The pie chart visually represents the distribution of students across these grades. The segments are
 1876 color-coded for each grade, with Grade 1 in red, Grade 2 in blue, Grade 3 in green, Grade 4 in
 1877 orange, and Grade 5 in purple. The chart provides a clear visual representation of the number of
 1878 students in each grade at the elementary school.

1879 **Query-relevant Captions (Qwen2.5-VL-3B):**

1880 The pie chart below represents the number of each grade at a United States elementary school. What
 1881 is the percentage of Grade 2? The answer should be a percentage between 0 and 100.

1884 Table 22: **Case Study with Qwen2.5-VL-3B.** Additional visual details that are relevant to the
 1885 question but are only generated by MLLMs with **VPO** are highlighted in red.
 1886

1887 **Image:**

**Question:**

Is the left graph isomorphic with the right graph? choice: (A) Yes (B) No

Query-relevant Captions (Qwen2.5-VL-3B w/ VPO):

The image consists of two graphs. The left graph is a connected graph with the following vertices and edges: A, B, C, D, E, F, G, and H. The edges are as follows: A is connected to H, A is connected to F, H is connected to E, B is connected to F, F is connected to E, E is connected to G, F is connected to G, and E is connected to D.

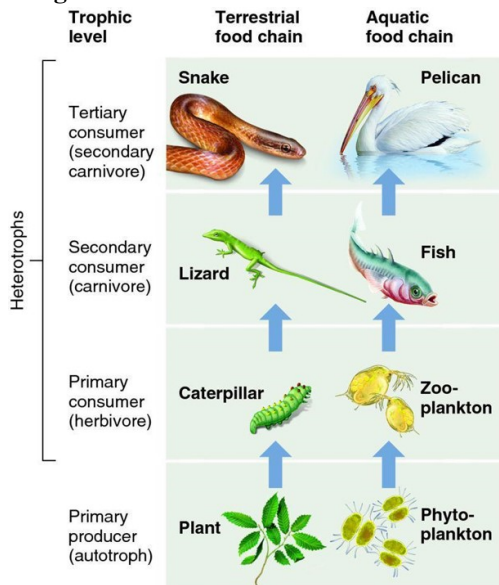
The right graph is a simple cycle graph with 8 vertices, labeled as 1, 2, 3, 4, 5, 6, 7 and 8 and edges connecting each vertex to the next in a circular manner.

Based on the description, the left graph is not isomorphic to the right graph. The left graph has a more complex structure with multiple connections and a central node (E), while the right graph is a simple cycle with no such central node and a different number of vertices.

Query-relevant Captions (Qwen2.5-VL-3B):

The left graph is a graph with 8 vertices and 10 edges. The right graph is a graph with 8 vertices and 8 edges. The left graph is not isomorphic to the right graph.

Table 23: **Case Study with Qwen2.5-VL-3B.** Additional visual details that are relevant to the question but are only generated by MLLMs with VPO are highlighted in red.

Image:

Question: Hint: Please answer the question and provide the correct option letter, e.g., A, B, C, D, at the end. Question: What happens to fish if pelicans increase? Choices: (A) decrease (B) nothing (C) increase (D) none of the above

Query-relevant Captions (Qwen2.5-VL-3B w/ VPO):

1944 The image depicts a food chain diagram showing the trophic levels and different types of consumers
 1945 in both terrestrial and aquatic environments. Here is a detailed description of the image:
 1946

1. **Trophic Level:**

- **Primary producer (autotroph):** This level includes plants and phytoplankton, which are the base of the food chain.
- **Primary consumer (herbivore):** This level includes caterpillars and zooplankton, which feed on the primary producers.
- **Secondary consumer (carnivore):** This level includes lizards and fish, which feed on the primary consumers.
- **Tertiary consumer (secondary carnivore):** This level includes snakes and pelicans, which feed on the secondary consumers.

2. **Terrestrial food chain:**

- **Primary producer (autotroph):** Plant
- **Primary consumer (herbivore):** Caterpillar
- **Secondary consumer (carnivore):** Lizard
- **Tertiary consumer (secondary carnivore):** Snake

3. **Aquatic food chain:**

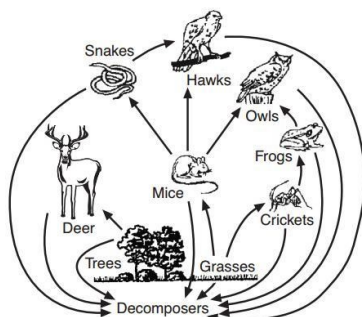
- **Primary producer (autotroph):** Phytoplankton
- **Primary consumer (herbivore):** Zooplankton
- **Secondary consumer (carnivore):** Fish
- **Tertiary consumer (secondary carnivore):** Pelican

The image also shows arrows indicating the direction of energy flow from one trophic level to the next, emphasizing the flow of energy through different ecosystems.

Query-relevant Captions (Qwen2.5-VL-3B): The image shows a food chain diagram with two types of food chains: terrestrial and aquatic. The terrestrial food chain includes a caterpillar, lizard, fish, and snake, with the caterpillar being the primary producer and the snake being the tertiary consumer. The aquatic food chain includes zooplankton, phytoplankton, fish, and a pelican, with the zooplankton being the primary producer and the pelican being the tertiary consumer.

Table 24: **Case Study with Qwen2.5-VL-3B.** Additional visual details that are relevant to the question but are only generated by MLLMs with **VPO** are highlighted in red.

Image:



Question:

Hint: Please answer the question and provide the correct option letter, e.g., A, B, C, D, at the end.
 Question: If frogs were removed from this environment what animal would potentially see an increase in its population? Choices:(A) crickets (B) deer (C) snakes (D) hawks

Query-relevant Captions (Qwen2.5-VL-3B w/ VPO):

1998 The image is a food web diagram depicting various organisms and their interactions within an
 1999 ecosystem. The diagram includes the following elements:

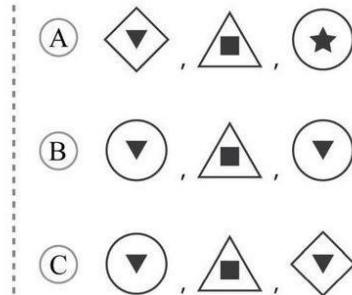
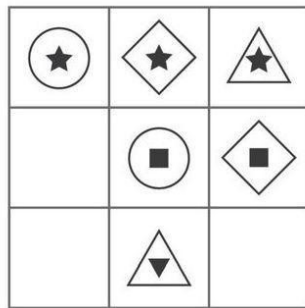
2000 • **Deer** (at the bottom left) consuming **Trees**.
 2001 • **Mice** (in the center) consuming **Grasses**.
 2002 • **Crickets** (in the center right) consuming **Grasses**.
 2003 • **Snakes** (at the top left) consuming **Mice**.
 2004 • **Hawks** (at the top center) consuming **Snakes**.
 2005 • **Owls** (at the top right) consuming **Mice**.
 2006 • **Frogs** (in the center right) consuming **Crickets**.
 2007 • **Decomposers** (at the bottom center) breaking down organic matter.

2008 The arrows indicate the direction of energy flow from one organism to another, showing the
 2009 relationships between the different species in the ecosystem.

2010 **Query-relevant Captions (Qwen2.5-VL-3B):** The image is a food web diagram depicting various
 2011 organisms and their interactions within an ecosystem. It includes a deer, trees, grasses, mice, crickets,
 2012 frogs, hawks, and owls. The arrows indicate the direction of energy flow from producers (trees and
 2013 grasses) to consumers (deer, mice, crickets, frogs, hawks, and owls), and decomposers
 2014 (decomposers). The diagram shows how energy moves through the ecosystem, with each organism
 2015 feeding on others, and how the removal of frogs could potentially lead to an increase in the
 2016 population of crickets, as they are a primary food source for frogs.

2017 Table 25: **Case Study with Qwen2.5-VL-32B.** Additional visual details that are relevant to the
 2018 question but are only generated by MLLMs with **VPO** are highlighted in **red**.

2019 **Image:**



2025 **Question:**

2026 Hint: Please answer the question and provide the correct option letter, e.g., A, B, C, D, at the end.
 2027 Question: Which option is correct? Choices: (A) A (B) B (C) C

2028 **Query-relevant Captions (Qwen2.5-VL-32B w/ VPO):**

2052
 2053 The image presents a logic puzzle involving patterns and shapes. Here is a detailed description of the
 2054 image:
 2055

2056 **Left Side: Grid with Shapes**
 2057

- 2058 • The grid is a 3x3 matrix.
 2059
- 2058 • Each cell contains a shape with a specific pattern or design.
 2059
- 2058 • The shapes include circles, diamonds, and triangles, each with different internal designs
 2059 (e.g., stars, squares, etc.).

2060 *Row 1:*

2061 1. Cell 1: A circle with a star inside.
 2062 2. Cell 2: A diamond with a star inside.
 2063 3. Cell 3: A triangle with a star inside.

2064 *Row 2:*

2065 1. **Cell 1: Empty.**
 2066 2. Cell 2: A circle with a square inside.
 2067 3. Cell 3: A diamond with a square inside.

2068 *Row 3:*

2069 1. **Cell 1: Empty.**
 2070 2. Cell 2: A triangle with a downward arrow inside.
 2071 3. **Cell 3: Empty.**

2072 **Right Side: Multiple Choice Options**

2073 There are three options labeled A, B, and C. Each option shows a sequence of three shapes. The task
 2074 is to determine the correct pattern that fits the logic of the grid.

2075 *Option A:*

2076 1. A diamond with a downward arrow inside.
 2077 2. A triangle with a square inside.
 2078 3. A circle with a star inside.

2079 *Option B:*

2080 1. A diamond with a downward arrow inside.
 2081 2. A triangle with a square inside.
 2082 3. A circle with a downward arrow inside.

2083 *Option C:*

2084
 2085
 2086
 2087
 2088
 2089
 2090
 2091
 2092
 2093
 2094
 2095
 2096
 2097
 2098
 2099
 2100
 2101
 2102
 2103
 2104
 2105

2106
 2107 1. A diamond with a downward arrow inside.
 2108 2. A triangle with a square inside.
 2109 3. A diamond with a downward arrow inside.
 2110

2111 **Analysis of the Grid Patterns**

2112 *Column-wise Observation:*

- 2113 • **Column 1:**
 - 2114 – Row 1: Circle with a star.
 - 2115 – Row 2: Empty.
 - 2116 – Row 3: Empty.
- 2117 • **Column 2:**
 - 2118 – Row 1: Diamond with a star.
 - 2119 – Row 2: Circle with a square.
 - 2120 – Row 3: Triangle with a downward arrow.
- 2121 • **Column 3:**
 - 2122 – Row 1: Triangle with a star.
 - 2123 – Row 2: Diamond with a square.
 - 2124 – Row 3: Empty (to be determined).

2125 *Row-wise Observation:*

- 2126 • **Row 1:** Circle (star), Diamond (star), Triangle (star)
- 2127 • **Row 2:** Empty, Circle (square), Diamond (square)
- 2128 • **Row 3:** Empty, Triangle (downward arrow), ? (to be determined)

2129 *Shape Progression:*

- 2130 • The shapes in each row and column follow a specific order: Circle → Diamond → Triangle.
- 2131 • The internal designs also follow a pattern: Star → Square → Downward Arrow.

2132 **Query-relevant Captions (Qwen2.5-VL-32B):**

2133 The image consists of two main sections:

2134 **Left Section:**

- 2135 • A 3x3 grid with various shapes and patterns.
- 2136 • The grid contains:
 - 2137 – A circle with a star inside in the top-left cell.
 - 2138 – A diamond with a star inside in the top-middle cell.
 - 2139 – A triangle with a star inside in the top-right cell.
 - 2140 – A circle with a square inside in the middle-left cell.
 - 2141 – A diamond with a square inside in the middle-middle cell.
 - 2142 – A triangle with a square inside in the middle-right cell.
 - 2143 – A triangle with a downward-pointing arrow inside in the bottom-left cell.
 - 2144 – The bottom-middle and bottom-right cells are empty.

2160
2161
2162
2163
2164
2165
2166
2167
2168
2169
2170
2171
2172
2173
2174
2175
2176
2177
2178
2179
2180
2181
2182
2183
2184
2185
2186
2187
2188
2189
2190
2191
2192
2193
2194
2195
2196
2197
2198
2199
2200
2201
2202
2203
2204
2205
2206
2207
2208
2209
2210
2211
2212
2213

Right Section:

- Three options labeled A, B, and C.
- Each option contains three shapes:
 - **Option A:** A diamond with a downward-pointing arrow inside, a triangle with a square inside, and a circle with a star inside.
 - **Option B:** A circle with a downward-pointing arrow inside, a triangle with a square inside, and another circle with a downward-pointing arrow inside.
 - **Option C:** A circle with a downward-pointing arrow inside, a triangle with a square inside, and a diamond with a downward-pointing arrow inside.

The task appears to involve identifying a pattern or sequence based on the shapes and their internal symbols in the grid and selecting the correct option from the choices provided.

Table 26: **Case Study with Qwen2.5-VL-32B.** Additional visual details that are relevant to the question but are only generated by MLLMs with **VPO** are highlighted in **red**.

Image:

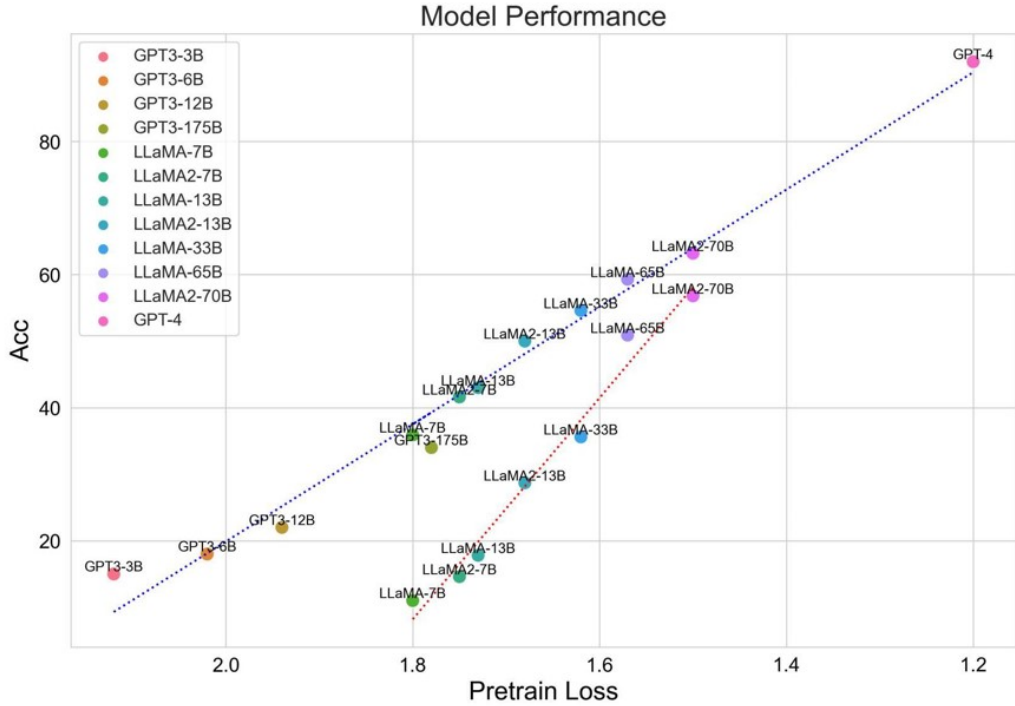


Figure 2: The performance of SFT (blue lines) and ICL (red lines) settings on GSM8K. GPT-4 states they use some part of the GSM8K data in pre-training, and suggest others consider its performance between SFT and ICL.

Question:

Hint: Please answer the question requiring an integer answer and provide the final value, e.g., 1, 2, 3, at the end. Question: How many models in the figure achieve an Acc score greater than 60?

Query-relevant Captions (Qwen2.5-VL-32B w/ VPO):

2214
 2215 The image is a scatter plot titled "**Model Performance**," which compares the performance of
 2216 various large language models on a specific task, likely related to the GSM8K dataset. The plot uses
 2217 different colors and line styles to distinguish between models and their training settings. Here is a
 2218 detailed description of the image:
 2219

Title and Labels:

2220
 2221

- **Title:** "Model Performance"
- **X-axis:** Labeled "Pretrain Loss," ranging from approximately 1.2 to 2.0.
- **Y-axis:** Labeled "ACC" (presumably short for Accuracy), ranging from 0 to 80.

 2222

Legend:

2223 The legend on the left side lists various models and their corresponding colors and markers:

2224
 2225

- GPT3-3B (pink), GPT3-6B (orange), GPT3-12B (yellow), GPT3-175B (dark green)
- LLaMA-7B (light green), LLaMA2-7B (teal), LLaMA-13B (dark teal), LLaMA2-13B
 2226 (light blue)
- LLaMA-33B (blue), LLaMA-65B (purple), LLaMA2-70B (pink), GPT-4 (dark pink)

 2227

Line Styles:

2228
 2229

- **Blue Lines:** Represent the SFT (Supervised Fine-Tuning) setting.
- **Red Lines:** Represent the ICL (In-Context Learning) setting.
- Dotted lines connect points for each model, showing trends in performance.

 2230

Data Points:

2231 Each model is represented by a series of points on the plot, with the position determined by:

2232
 2233

- **X-axis (Pretrain Loss):** Lower values indicate better pretraining.
- **Y-axis (ACC):** Higher values indicate better accuracy.

 2234

Key Observations:

2235
 2236

1. **GPT-4 Performance:**
 - GPT-4 (dark pink) achieves the highest accuracy (ACC) score, well above 60, and has a low pretraining loss.
 - It is plotted as a single point at the top-right of the graph.
2. **LLaMA and LLaMA2 Models:**
 - Various LLaMA and LLaMA2 models (e.g., LLaMA-7B, LLaMA2-7B, LLaMA-13B, etc.) are scattered across the plot.
 - Larger models (e.g., LLaMA2-70B) tend to have higher accuracy scores.
3. **GPT3 Models:**
 - GPT3 models (GPT3-3B, GPT3-6B, GPT3-12B, GPT3-175B) are plotted with lower accuracy scores compared to LLaMA and LLaMA2 models.
 - GPT3-175B performs better than smaller GPT3 models but still lags behind the larger LLaMA models.
4. **Accuracy Threshold (ACC > 60):**
 - Models achieving an ACC score greater than 60 are primarily from the LLaMA2 series and GPT-4.
 - Notable models include:
 - LLaMA2-70B
 - LLaMA2-65B
 - LLaMA2-33B
 - GPT-4

Text Caption:

2237 The caption below the figure provides additional context:

2238
 2239

- **Figure 2:** Describes the performance of SFT (blue lines) and ICL (red lines) settings on
 2240 GSM8K.
- Notes that GPT-4 uses some part of the GSM8K data in pretraining and suggests its
 2241 performance lies between SFT and ICL.⁴²

2268

2269

2270

2271

2272

2273

2274

2275

2276

2277

2278

2279

2280

2281

2282

2283

2284

2285

2286

2287

2288

2289

2290

2291

2292

2293

2294

2295

2296

2297

2298

2299

2300

2301

2302

2303

2304

2305

2306

2307

2308

2309

2310

2311

2312

2313

2314

2315

2316

2317

2318

2319

2320

2321

Query-relevant Captions (Qwen2.5-VL-32B):

The image is a scatter plot titled "**Model Performance**." It compares the performance of various large language models on a task, likely related to the GSM8K dataset, based on two metrics: "ACC" (accuracy) on the y-axis and "Pretrain Loss" on the x-axis. The models are represented by different colored dots, and the legend on the left identifies each model by name and color. The models include various versions of GPT-3 (3B, 6B, 12B, 175B), LLaMA (7B, 13B, 33B, 65B, 70B), LLaMA2 (7B, 13B, 33B, 65B, 70B), and GPT-4.

Key Features:**1. Axes:**

- **Y-axis (ACC):** Ranges from 0 to 80, representing accuracy scores.
- **X-axis (Pretrain Loss):** Ranges from 1.2 to 2.0, representing pretraining loss values.

2. Models:

- Each model is represented by a colored dot, with the model name labeled near the dot.
- Models include the GPT-3 series, LLaMA series, LLaMA2 series, and GPT-4.

3. Trends:

- There are two sets of lines:
 - **Blue lines (SFT settings):** Represent the performance of models under supervised fine-tuning (SFT).
 - **Red lines (ICL settings):** Represent the performance of models under in-context learning (ICL).
- GPT-4 is shown as a single point, suggesting its unique position in the performance landscape.

4. Legend:

- The legend on the left provides a color-coded list of models, including:
 - GPT-3 variants: 3B, 6B, 12B, 175B
 - LLaMA variants: 7B, 13B, 33B, 65B, 70B
 - LLaMA2 variants: 7B, 13B, 33B, 65B, 70B
 - GPT-4

5. Caption:

- The caption explains that the figure shows the performance of SFT (blue lines) and ICL (red lines) settings on GSM8K.
- It notes that GPT-4 uses some part of the GSM8K data in pretraining and suggests its performance lies between SFT and ICL.

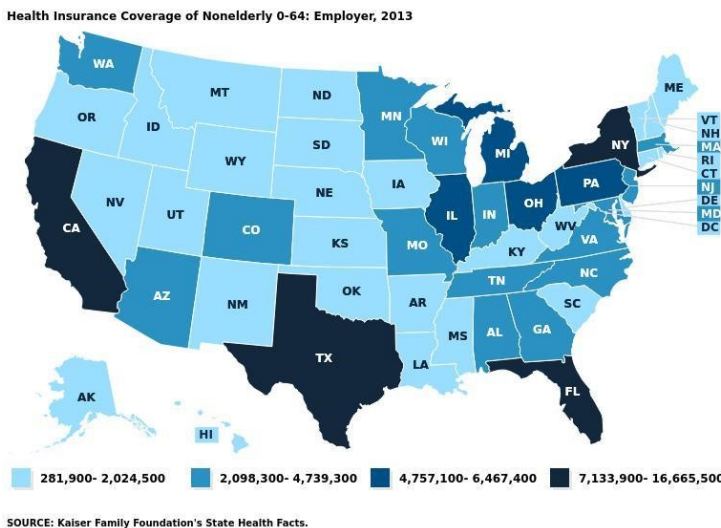
Question:

The question asks how many models in the figure achieve an ACC score greater than 60. The task is to count the number of models that meet this criterion based on the scatter plot. However, the instruction is to describe the image without answering the question.

Table 27: **Case Study with Qwen2.5-VL-32B.** Additional visual details that are relevant to the question but are only generated by MLLMs with **VPO** are highlighted in red.

Image:

2322
2323
2324
2325
2326
2327
2328
2329
2330
2331
2332
2333
2334
2335
2336
2337
2338
2339
2340
2341
2342



Question:

Hint: Please answer the question and provide the correct option letter, e.g., A, B, C, D, at the end.

Question: Does South Carolina have the highest value in the South? Choices: (A) Yes (B) No

Query-relevant Captions (Qwen2.5-VL-32B w/ VPO):

The image is a choropleth map of the United States, depicting the distribution of health insurance coverage for nonelderly individuals (ages 0–64) through employer-sponsored plans in 2013. Here is a detailed description of the image:

Title and Subtitle:

- **Title:** “Health Insurance Coverage of Nonelderly 0–64: Employer, 2013”
- This indicates that the map shows the number of nonelderly individuals (aged 0–64) who had employer-sponsored health insurance in 2013.

Color Coding:

The map uses a gradient of blue shades to represent different ranges of employer-sponsored health insurance coverage. The legend at the bottom explains the color coding:

- **Lightest Blue:** 281,900 – 2,024,500
- **Light Blue:** 2,098,300 – 4,739,300
- **Medium Blue:** 4,757,100 – 6,467,400
- **Darkest Blue:** 7,133,900 – 16,665,500

State Colors:

- **Darkest Blue (Highest Coverage):** States in this category include California (CA), New York (NY), Texas (TX), and Florida (FL). These states have the highest number of nonelderly individuals with employer-sponsored health insurance.
- **Medium Blue:** States like Illinois (IL), Ohio (OH), Pennsylvania (PA), and Michigan (MI) fall into this category.
- **Light Blue:** States such as Colorado (CO), Arizona (AZ), and Tennessee (TN) are in this range.
- **Lightest Blue (Lowest Coverage):** States with the lowest coverage include Alaska (AK), Hawaii (HI), Wyoming (WY), and several others in the Midwest and Northeast.

2371
2372
2373
2374
2375

2376

2377

South Region Analysis:

2378

2379

2380

2381

2382

2383

2384

2385

2386

2387

2388

2389

2390

2391

2392

2393

2394

2395

2396

2397

2398

2399

2400

2401

2402

2403

2404

2405

2406

2407

2408

2409

2410

2411

2412

2413

2414

2415

2416

2417

2418

2419

2420

2421

2422

2423

2424

2425

2426

2427

2428

2429

- **Highest Value in the South:** The darkest blue states in the South are Texas (TX) and Florida (FL), indicating they have the highest employer-sponsored health insurance coverage in the region.
- **South Carolina (SC):** South Carolina is colored in a light blue shade, indicating it falls into the range of 2,098,300 – 4,739,300. This is not the highest value in the South.

Other Observations:

- **Northeast:** New York (NY) and Pennsylvania (PA) have high coverage, with NY in the darkest blue category.
- **Midwest:** States like Illinois (IL) and Ohio (OH) have medium to high coverage.
- **West:** California (CA) stands out with the darkest blue, indicating the highest coverage in the West.

Source:

The map is sourced from the Kaiser Family Foundation's State Health Facts, as noted at the bottom of the image.

Question Analysis:

The question asks whether South Carolina has the highest value in the South. Based on the map:

- South Carolina is in a light blue category, not the darkest blue.
- The highest values in the South are represented by Texas and Florida, which are in the darkest blue category.

Query-relevant Captions (Qwen2.5-VL-32B):

The image is a choropleth map of the United States, illustrating the distribution of health insurance coverage for nonelderly individuals aged 0–64 through employer-sponsored plans in 2013. The map uses varying shades of blue to represent different ranges of coverage numbers across the states.

The legend at the bottom indicates four categories of coverage:

- **Lightest Blue:** 281,900 – 2,024,500
- **Light Blue:** 2,098,300 – 4,739,300
- **Medium Blue:** 4,757,100 – 6,467,400
- **Darkest Blue:** 7,133,900 – 16,665,500

Key observations from the map:

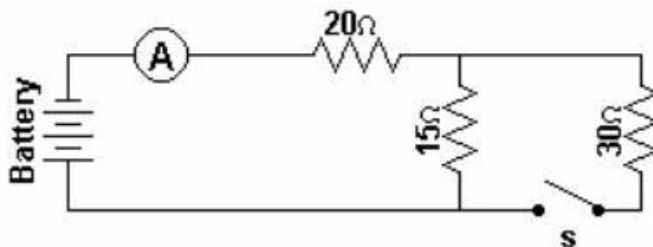
- States like California (CA), Texas (TX), and Florida (FL) are shaded in the darkest blue, indicating the highest range of employer-sponsored health insurance coverage.
- Many states in the Midwest and West are shaded in lighter blues, indicating lower coverage numbers.
- The source of the data is cited as the Kaiser Family Foundation's State Health Facts.

The question asks whether South Carolina (SC) has the highest value in the South. The map shows South Carolina in a light blue shade, indicating it falls into the second-lowest category of coverage.

Table 28: **Case Study with Qwen2.5-VL-32B.** Additional visual details that are relevant to the question but are only generated by MLLMs with VPO are highlighted in red.

Image:

2430
2431
2432
2433
2434
2435
2436
2437
2438



2439
2440
2441
2442

Question:

<image 1>A battery, an ammeter, three resistors, and a switch are connected to form the simple circuit shown above. When the switch is closed what would happen to the potential difference across the 15 ohm resistor?

2443
2444
2445
2446

Query-relevant Captions (Qwen2.5-VL-32B w/ VPO):

The image depicts an electrical circuit involving a battery, an ammeter, three resistors, and a switch. Here is a detailed description of the components and their arrangement:

Components in the Circuit:

2447
2448
2449
2450

1. Battery:

- Located on the left side of the circuit.
- Serves as the power source, providing the electromotive force (EMF) to the circuit.

2451
2452
2453
2454

2. Ammeter (A):

- Placed immediately after the battery.
- Used to measure the current flowing through the circuit.
- It is connected in series with the rest of the circuit.

2455
2456
2457
2458

3. Resistors:

- There are three resistors with the following resistances:
 - A $20\ \Omega$ resistor
 - A $15\ \Omega$ resistor
 - A $30\ \Omega$ resistor
- The resistors are connected in a combination of series and parallel configurations.

2462
2463
2464
2465

4. Switch (S):

- Located on the right side of the circuit.
- Controls the flow of current in the circuit. When closed, the circuit is complete, and current can flow.

2466
2467
2468
2469
2470
2471
2472
2473

Circuit Configuration:

- The $20\ \Omega$ resistor is connected in series with the rest of the circuit.
- The $15\ \Omega$ and $30\ \Omega$ resistors are connected in parallel.
- The parallel combination is then connected in series with the $20\ \Omega$ resistor.
- The ammeter is in series with all the resistors, measuring the total current.
- The switch is placed after the parallel combination, completing the circuit when closed.

2474
2475
2476
2477
2478
2479
2480
2481
2482
2483

2484

2485

2486

2487

2488

2489

2490

2491

2492

2493

2494

2495

2496

2497

2498

2499

2500

2501

2502

2503

2504

2505

2506

2507

2508

2509

2510

2511

2512

2513

2514

2515

2516

2517

2518

2519

2520

2521

2522

2523

2524

2525

2526

2527

2528

2529

2530

2531

2532

2533

2534

2535

2536

2537

Path of Current:

1. Current flows from the positive terminal of the battery.
2. It passes through the ammeter.
3. It then encounters the $20\ \Omega$ resistor.
4. After the $20\ \Omega$ resistor, the current splits:
 - One part flows through the $15\ \Omega$ resistor.
 - The other part flows through the $30\ \Omega$ resistor.
5. The currents recombine after the parallel branch.
6. The combined current continues through the rest of the circuit and returns to the battery.

Analysis of Potential Difference:

- When the switch is closed, current flows through the circuit and potential differences develop across each resistor.
- The $15\ \Omega$ and $30\ \Omega$ resistors are in parallel.
- In a parallel configuration, the potential difference across each branch is the same.
- Therefore, the potential difference across the $15\ \Omega$ resistor is equal to that across the $30\ \Omega$ resistor.

Query-relevant Captions (Qwen2.5-VL-32B):

The image depicts a simple electrical circuit consisting of the following components:

- **Battery:** A power source labeled as "Battery" is shown on the left side of the circuit.
- **Ammeter (A):** A device used to measure the current in the circuit is connected in series with the battery.
- **Resistors:** Three resistors are present in the circuit:
 - A $20\ \Omega$ resistor is connected in series with the ammeter.
 - A $15\ \Omega$ resistor is connected in parallel with a $30\ \Omega$ resistor.
- **Switch (S):** A switch is placed in the circuit, which can be opened or closed to control the flow of current.
- **Wires:** The components are connected by wires to form a complete circuit.

Circuit Configuration:

- The $20\ \Omega$ resistor is in series with the ammeter and the battery.
- The $15\ \Omega$ resistor and the $30\ \Omega$ resistor are connected in parallel with each other.
- The switch is placed in the branch that includes the parallel combination of the $15\ \Omega$ and $30\ \Omega$ resistors.

Key Observations:

- When the switch is closed, the parallel combination of the $15\ \Omega$ and $30\ \Omega$ resistors will be active, allowing current to flow through both resistors.
- The ammeter measures the total current flowing through the circuit.

This description provides a detailed overview of the circuit's components and their arrangement.

Table 29: **Case Study with Qwen2.5-VL-32B.** Additional visual details that are relevant to the question but are only generated by MLLMs with **VPO** are highlighted in red.

Image:

2538

2539

2540

2541

2542

2543

2544

2545

2546

2547

2548

2549

2550

2551

2552

2553

2554

2555

2556

2557

2558

2559

2560

2561

2562

2563

2564

2565

2566

2567

2568

2569

2570

2571

2572

2573

2574

2575

2576

2577

2578

2579

2580

2581

2582

2583

2584

2585

2586

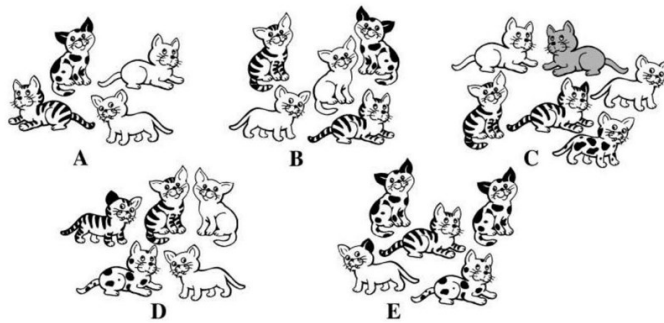
2587

2588

2589

2590

2591

**Question:**

Hint: Please answer the question and provide the correct option letter, e.g., A, B, C, D, at the end. Question: Misty the cat has five kittens: two of them are striped, one spotty, the rest of them are absolutely white. In which picture can we see the kittens of Misty, knowing that the ears of one of them are of different colour? Choices: (A) A (B) B (C) C (D) D (E) E

Query-relevant Captions (Qwen2.5-VL-32B w/ VPO):

The image presents a multiple-choice question involving illustrations of cats. Here is a detailed description of the image:

Overall Structure:

- The image contains **five labeled sections**, each representing a different option: **A, B, C, D, and E**.
- Each section features a group of cartoon-style cat illustrations.
- The question describes a specific scenario about a cat named Misty who has five kittens with particular characteristics.
- The task is to identify which section correctly represents Misty's kittens based on the given clues.

Clues from the Question:

1. Misty has five kittens.
2. Two of the kittens are striped.
3. One kitten is spotty.
4. The rest (two kittens) are absolutely white.
5. One of the kittens has ears of a different color.

Analysis of Each Section:**Section A:**

- 1 striped, 1 spotty, 2 white kittens.
- No kitten has ears of a different color.

Section B:

- 2 striped, 1 spotty, 2 white kittens.
- No kitten with differently colored ears.

Section C:

- 2 striped, 1 spotty, 2 white, 1 gray kittens.
- One kitten has ears of a different color.

2592

2593

2594

2595

2596

2597

2598

2599

2600

2601 **Section D:**

- 2 striped, 1 spotty, 2 white kittens.
- One kitten has ears of a different color.

2602 **Section E:**

- 1 striped, 3 spotty, 1 white kittens.
- One kitten has ears of a different color.

2603 **Query-relevant Captions (Qwen2.5-VL-32B):**

2604 The image shows five groups of cartoon-style cats, each labeled with a letter (A, B, C, D, E). Each
 2605 group contains multiple cats with various patterns and colors, including striped, spotty, and
 2606 solid-colored cats. The cats are depicted in different poses, such as sitting, lying down, or standing.
 2607 The question asks to identify the group that matches the description of Misty's kittens, which
 2608 includes two striped, one spotty, and two white kittens, with one having differently colored ears.

2609 **Detailed Description of Each Group:**

- **Group A:** Contains cats with striped and spotty patterns. Some cats have differently colored ears.
- **Group B:** Features cats with striped and solid-colored patterns. No cats have differently colored ears.
- **Group C:** Includes cats with striped, spotty, and solid-colored patterns. No cats have differently colored ears.
- **Group D:** Shows cats with striped and solid-colored patterns. No cats have differently colored ears.
- **Group E:** Contains cats with striped, spotty, and solid-colored patterns. No cats have differently colored ears.

2610 The task is to identify the group that matches the specific description of Misty's kittens.

2611 **Misty's Kittens:**

- Two striped kittens
- One spotty kitten
- Two white (solid-colored) kittens
- One kitten has differently colored ears

2612 **Conclusion:** Only **Group A** meets all the criteria, including the presence of differently colored ears.

2628

2629

2630

2631

2632

2633

2634

2635

2636

2637

2638

2639

2640

2641

2642

2643

2644

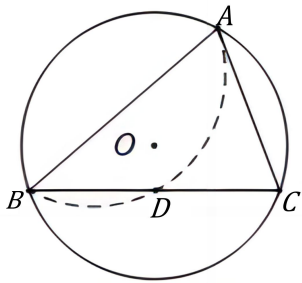
2645

A

2646
 2647
 2648
 2649
 2650
 2651
 2652
 2653
 2654
 2655
 2656
 2657
 2658
 2659
 2660
 2661
 2662
 2663
 2664
 2665
 2666
 2667
 2668
 2669
 2670
 2671
 2672
 2673
 2674
 2675
 2676
 2677
 2678
 2679
 2680
 2681
 2682
 2683
 2684
 2685
 2686
 2687
 2688
 2689
 2690
 2691
 2692
 2693
 2694
 2695
 2696
 2697
 2698
 2699

Table 30: **Reasoning Case Study with Qwen2.5-VL-3B.** Additional visual details that are relevant to the question but are only generated by MLLMs with VPO are highlighted in red. Reasoning process that show confusing and contradiction are highlighted in brown.

Image:



Question:

O is the circumcircle of $\triangle ABC$, with $AB = BC = 16$. The arc AB is folded down along the chord AB to intersect BC at point D . If point D is the midpoint of BC , what is the length of AC ?

Query-relevant Captions (Qwen2.5-VL-3B w/ VPO):

The image is a geometric diagram of a triangle $\triangle ABC$ inscribed in a circle with center O . The diagram shows the following elements:

- Points A , B , and C are the vertices of the triangle.
- Point O is the center of the circumcircle of $\triangle ABC$.
- Line segment AB is a chord of the circle.
- Line segment BC is another chord of the circle.
- Point D is a point on the circle such that the arc AB is folded down along the chord AB to intersect BC at D .
- The diagram includes a dashed line segment AD and a dashed line segment BD .

The image does not provide any numerical values or specific measurements, and it does not contain any text or additional information. The focus is purely on the geometric relationships and the diagram itself.

Query-relevant Captions (Qwen2.5-VL-3B):

The image shows a circle with center O and points A , B , and C on its circumference. The line segment AB is a diameter of the circle, and the arc AB is folded down along the chord AB to intersect BC at point D . Point D is the midpoint of BC .

Reasoning Result of R1-7B (captions from Qwen2.5-VL-3B w/ VPO):

Alright, let me try to figure out this geometry problem step by step. So, we have triangle ABC inscribed in a circle with center O . AB and BC are both 16 units long, making it an isosceles triangle with $AB = BC$. The diagram shows that when arc AB is folded along chord AB , it intersects BC at point D , which is the midpoint of BC . So, $BD = DC = 8$ units.

First, I need to visualize this. Since ABC is isosceles with $AB = BC$, the base is AC , and the two equal sides are AB and BC . The circle is the circumcircle, so all three vertices lie on the circumference.

When the arc AB is folded along AB , point D is where the fold intersects BC . Since D is the midpoint, $BD = DC = 8$. Folding along AB suggests that point D is the reflection of point C over the line AB . But since D lies on BC , maybe there's some symmetry here.

I think I should consider the properties of the circumcircle. In a triangle inscribed in a circle, the perpendicular bisectors of the sides meet at the center O . Since $AB = BC$, the triangle is isosceles, so the median from B to AC should also be the altitude and the angle bisector.

Wait, but we're dealing with a fold along AB . When you fold along AB , point C would map to some point on BC . Since D is the midpoint, maybe there's a reflection involved here. Let me try to see if triangle ABD is congruent or similar to another triangle.

2700

2701

2702

2703

2704

2705

2706

2707

2708

2709

2710

2711

2712

2713

2714

2715

2716

2717

2718

2719

2720

2721

2722

2723

2724

2725

2726

2727

2728

2729

2730

2731

2732

2733

2734

2735

2736

2737

2738

2739

2740

2741

2742

2743

2744

2745

2746

2747

2748

2749

2750

2751

2752

2753

Alternatively, maybe using the Law of Cosines would help. Let's denote angle at B as angle ABC . Since $AB = BC = 16$, the triangle is isosceles, so angles at A and C are equal. But when we fold arc AB over AB , point D is created on BC . Since D is the midpoint, perhaps there's a relationship between the angles or the lengths.

Wait, another approach: when you fold along AB , point C maps to D . So, AD should equal AC because reflection preserves distances. So, $AD = AC$. Also, since D is the midpoint of BC , $BD = DC = 8$. So, in triangle ABD , we have $AB = 16$, $BD = 8$, and $AD = AC$.

So, triangle ABD has sides $AB = 16$, $BD = 8$, and $AD = AC = x$. Maybe I can apply the Law of Cosines here. Let's denote AC as x . Then, $AD = x$ as well.

In triangle ABD :

$$AB^2 + BD^2 - 2 \cdot AB \cdot BD \cdot \cos(\angle ABD) = AD^2$$

Which is:

$$16^2 + 8^2 - 2 \cdot 16 \cdot 8 \cdot \cos(\angle ABD) = x^2$$

$$256 + 64 - 256 \cdot \cos(\angle ABD) = x^2$$

$$320 - 256 \cdot \cos(\angle ABD) = x^2$$

But I don't know angle ABD . Maybe I can relate it to the original triangle ABC . Since ABC is isosceles with $AB = BC = 16$, angle ABC is equal to angle BAC and angle BCA ? Wait, no, in an isosceles triangle, the angles opposite the equal sides are equal. So, since $AB = BC$, the angles opposite them, which would be angle ACB and angle BAC , are equal.

Wait, no, in triangle ABC , $AB = BC = 16$, so the sides opposite angles at C and A respectively. So, angle at C (angle ACB) equals angle at A (angle BAC). Let's denote angle BAC as θ , so angle ACB is also θ , and angle ABC is $180 - 2\theta$ degrees.

When we fold along AB , point C maps to D on BC . So, the reflection over AB takes point C to D . Therefore, $AD = AC$ and angle $BAD = \angle BAC = \theta$.

Wait, but AD is equal to AC because reflection preserves length. So, triangle ABD has sides $AB = 16$, $BD = 8$, and $AD = AC = x$. Maybe I can use the Law of Cosines here as well.

Alternatively, maybe using the Law of Sines in triangle ABC . Since ABC is isosceles with $AB = BC = 16$, the circumradius can be found using the formula:

$$R = \frac{a}{2 \cdot \sin(A)}$$

Where a is the length of a side, and A is the opposite angle.

Wait, but I'm not sure if that's the right approach. Let me think again.

Since ABC is isosceles with $AB = BC = 16$, then angle at A equals angle at C . Let me denote angle at B as ϕ . So, in triangle ABC , angles are ϕ at B , and $(180 - \phi)/2$ at A and C each.

Now, when we fold along AB , point C is reflected over AB to point D on BC . So, $AD = AC$, and $BD = 8$, $DC = 8$.

So, in triangle ABD , $AB = 16$, $BD = 8$, $AD = x$.

2754 So, using the Law of Cosines on triangle ABD :

$$2755 \quad AB^2 + BD^2 - 2 \cdot AB \cdot BD \cdot \cos(\angle ABD) = AD^2$$

$$2756 \quad 16^2 + 8^2 - 2 \cdot 16 \cdot 8 \cdot \cos(\angle ABD) = x^2$$

$$2757 \quad 256 + 64 - 256 \cdot \cos(\angle ABD) = x^2$$

$$2758 \quad 320 - 256 \cdot \cos(\angle ABD) = x^2$$

2759 But angle ABD is the same as angle ABC , which is ϕ . So, $\cos(\angle ABD) = \cos(\phi)$.

2760 From triangle ABC , using the Law of Cosines:

$$2761 \quad AC^2 = AB^2 + BC^2 - 2 \cdot AB \cdot BC \cdot \cos(\phi)$$

$$2762 \quad x^2 = 16^2 + 16^2 - 2 \cdot 16 \cdot 16 \cdot \cos(\phi)$$

$$2763 \quad x^2 = 512 - 512 \cdot \cos(\phi)$$

2764 But from triangle ABD , we have $x^2 = 320 - 256 \cdot \cos(\phi)$

2765 So, setting them equal:

$$2766 \quad 512 - 512 \cdot \cos(\phi) = 320 - 256 \cdot \cos(\phi)$$

$$2767 \quad 512 - 320 = 512 \cdot \cos(\phi) - 256 \cdot \cos(\phi)$$

$$2768 \quad 192 = 256 \cdot \cos(\phi)$$

$$2769 \quad \cos(\phi) = \frac{192}{256} = \frac{3}{4}$$

2770 So, angle ϕ has cosine $\frac{3}{4}$. Now, substituting back into the equation for x^2 from triangle ABC :

$$2771 \quad x^2 = 512 - 512 \cdot \left(\frac{3}{4}\right)$$

$$2772 \quad x^2 = 512 - 384 = 128$$

$$2773 \quad x = \sqrt{128} = 8\sqrt{2}$$

2774 Wait, but this contradicts the initial thought that AC is $16\sqrt{2}$. Hmm, maybe I made a mistake in the reflection part. Let me check.

2775 Wait, when we fold along AB , point C maps to D on BC . So, AD should equal AC because reflection preserves distance. So, $AD = AC = x$.

2776 But in triangle ABD , we have $AB = 16$, $BD = 8$, $AD = x$.

2777 Using Law of Cosines:

$$2778 \quad 16^2 + 8^2 - 2 \cdot 16 \cdot 8 \cdot \cos(\angle ABD) = x^2$$

$$2779 \quad 256 + 64 - 256 \cdot \cos(\angle ABD) = x^2$$

$$2780 \quad 320 - 256 \cdot \cos(\angle ABD) = x^2$$

2781 But angle ABD is the same as angle ABC , which is ϕ . So, $\cos(\angle ABD) = \cos(\phi) = \frac{3}{4}$.

2782 Thus, $x^2 = 320 - 256 \cdot \left(\frac{3}{4}\right) = 320 - 192 = 128$

$$2783 \quad x = \sqrt{128} = 8\sqrt{2}$$

2784 Wait, so that would make $AC = 8\sqrt{2}$, not $16\sqrt{2}$ as the initial model response suggested. Hmm, so maybe the model response was incorrect.

2785 Alternatively, perhaps I made a mistake in assuming angle ABD is equal to angle ABC . Let me think again.

2808 In triangle ABC , angle ABC is at point B , between AB and BC . When we fold along AB , the
 2809 angle at B remains the same, but the direction changes. So, the angle ABD in triangle ABD is
 2810 actually angle between AB and BD , which is different from angle ABC .
 2811
 2812 Wait, no, BD is part of BC , so angle ABD is actually the same as angle ABC because BD is
 2813 along BC . So, maybe my initial assumption was correct.
 2814
 2815 Wait, but then according to this calculation, $AC = 8\sqrt{2}$, which is about 11.31, but given that AB
 2816 and BC are 16, that seems plausible.
 2817
 2818 Alternatively, maybe I should consider that when folding, the angle at D is a right angle. So, maybe
 2819 triangle ABD is a right triangle.
 2820
 2821 Wait, in the model response, they concluded that angle BAC is 90 degrees, which might not be
 2822 correct. Let me see.
 2823
 2824 If angle BAC is 90 degrees, then triangle ABC would be a right-angled isosceles triangle, making
 2825 $AC = AB \cdot \sqrt{2} = 16\sqrt{2}$. But according to my calculation, it's $8\sqrt{2}$. So, maybe the model response
 2826 was wrong.
 2827
 2828 Wait, perhaps the mistake is in assuming that $AD = AC$. When you fold along AB , point C maps
 2829 to D , so the distance from A to D should equal the distance from A to C , right? So, $AD = AC$. So,
 2830 that part seems correct.
 2831
 2832 Wait, but in the model response, they used Law of Cosines with angle BAC being 90 degrees, which
 2833 led to $AC = 16\sqrt{2}$. But according to my calculation, angle BAC is not necessarily 90 degrees, and
 2834 it's actually determined by the folding.
 2835
 2836 Wait, perhaps I should use the fact that in the folded diagram, $AD = AC$ because of reflection. So,
 2837 maybe triangle ABD is congruent to triangle ABC ? But no, because BD is only 8, not 16.
 2838
 2839 Alternatively, perhaps using coordinate geometry would help. Let me place point A at $(0,0)$, point B
 2840 at $(16,0)$, since $AB = 16$. Since ABC is isosceles with $AB = BC = 16$, point C would be
 2841 somewhere such that $BC = 16$.
 2842 ... (rest of the reasoning)
 2843 Therefore, the correct answer should be $AC = 8\sqrt{2}$, not $16\sqrt{2}$ as in the model response.
 2844
 2845 But wait, maybe I made a mistake in assuming angle ABD is equal to angle ABC . Let me think
 2846 again.
 2847
 2848 In triangle ABC , angle at B is ϕ , which we found $\cos(\phi) = \frac{3}{4}$. When folding along AB , the angle
 2849 at B remains the same, so angle ABD is indeed ϕ . Therefore, my calculation should be correct.
 2850
 2851 Therefore, the model response was incorrect, and the correct answer is $AC = 8\sqrt{2}$.
 2852
2853 Reasoning Result of R1-7B (captions from Qwen2.5-VL-3B):
 2854 Alright, so I'm trying to solve this geometry problem.
 2855
 2856 Let me read it again carefully.
 2857 We have triangle ABC with $AB = BC = 16$.
 2858
 2859 So, it's an isosceles triangle with AB and BC equal.
 2860
 2861 That means angles at A and C are equal, right?
 2862
 2863 Wait, no, actually, in triangle ABC, if $AB = BC$, then the base is AC, so the base angles at A and C
 2864 are equal.
 2865

2862 Hmm, but I'm not sure if that's important right now.
 2863 The problem mentions that the arc AB is folded down along the chord AB to intersect BC at point D.
 2864
 2865 And D is the midpoint of BC.
 2866
 2867 So, BC is 16, so BD and DC are each 8.
 2868
 2869 Got it.
 2870 We need to find the length of AC.
 2871 First, I should probably visualize the problem.
 2872
 2873 Let me draw a circle with center O, points A, B, and C on the circumference.
 2874
 2875 AB is a diameter, but wait, hold on.
 2876
 2877 The caption says the image shows a circle with center O and points A, B, C on the circumference.
 2878
 2879 The line segment AB is a diameter, and the arc AB is folded down along AB to intersect BC at D, which is the midpoint.
 2880 Wait, so AB is a diameter, which would mean that angle ACB is a right angle because any triangle inscribed in a semicircle is a right triangle.
 2881
 2882 But hold on, in the problem statement, it says $AB = BC = 16$.
 2883
 2884 If AB is a diameter, then AB would be the longest side, but BC is also 16, so that's interesting
 2885 because in a right triangle, the hypotenuse is the longest side.
 2886
 2887 So if AB is the diameter and a side of the triangle, then AB would be the hypotenuse.
 2888
 2889 But in the problem, $AB = BC$, so both would be legs, which can't be because in a right triangle, the
 2890 hypotenuse is longer than the legs.
 2891
 2892 Hmm, maybe AB isn't the diameter?
 2893 Wait, the initial caption says AB is a diameter, but the problem statement says $AB = BC = 16$.
 2894
 2895 That seems conflicting because if AB is a diameter, it should be longer than BC.
 2896
 2897 Maybe I misread the problem.
 2898
 2899 Let me check.
 2900 Wait, no, the problem says O is the circumcircle of triangle ABC.
 2901
 2902 So O is the circumradius.
 2903
 2904 If AB is a diameter, then the circumradius would be half of AB, which would make the circumradius 8.
 2905
 2906 But if AB is 16, then the circumradius is 8.
 2907
 2908 However, in that case, triangle ABC would have AB as the diameter, making angle ACB a right angle.
 2909
 2910 But in the problem, $AB = BC = 16$, so triangle ABC would have two sides equal to 16 and one side (AC) which we need to find.
 2911
 2912 But if angle C is 90 degrees, then AC would be the other leg, so $AC = BC = 16$, making it an
 2913 isosceles right triangle, so AC would be $16\sqrt{2}$.
 2914
 2915

2916 But wait, that seems too straightforward, and maybe that's the answer, but I'm not sure because the
 2917 folding part might complicate things.

2918 Wait, the problem mentions that the arc AB is folded down along AB to intersect BC at D, which is
 2920 the midpoint.

2921 So maybe the initial assumption that AB is a diameter isn't correct because when you fold the arc AB
 2922 down along AB, it intersects BC at D, which is the midpoint, so maybe AB isn't a diameter.

2924 **Hmm, now I'm confused.**

2926 Alternatively, let me try to think differently.

2928 Maybe AB isn't the diameter, but just a chord.

2930 So the circle has center O, and AB is a chord, not necessarily the diameter.

2932 Then, the arc AB is folded along AB, meaning reflecting the arc AB over the chord AB, which would
 2933 create a reflection of point C over AB, landing at point D on BC.
 2934 Since D is the midpoint of BC, which is 16, so $BD = DC = 8$.

2936 So, when you fold arc AB over AB, the reflection of C over AB is D, which lies on BC.

2938 So, perhaps triangle ABD is congruent to triangle ABC, but I'm not sure.

2940 Alternatively, maybe the reflection of C over AB is D, which is on BC.

2942 So, the distance from C to AB is the same as from D to AB, but since D is on BC, maybe we can use
 2943 some properties here.

2944 Wait, perhaps using coordinates would help.

2946 Let me try to place the points on a coordinate system.

2948 Let's place point B at the origin $(0,0)$.

2950 Since $AB = 16$, let me place point A at $(16, 0)$.

2952 Then, since AB is a chord of the circle, the center O is somewhere in the plane.

2954 Let me denote point C as (x, y) .

2956 Since $AB = BC = 16$, the distance from B to C is 16, so $\sqrt{x^2 + y^2} = 16$.

2958 Also, since ABC is a triangle, point C is somewhere not on AB.
 2959 Now, the arc AB is folded over AB, and it intersects BC at D, which is the midpoint of BC.

2961 So, since B is at $(0,0)$ and C is at (x,y) , the midpoint D is at $(\frac{x}{2}, \frac{y}{2})$.
 2962 When we fold the arc AB over AB, the reflection of point C over AB is point D.

2964 So, the reflection of point C over AB is D, which lies on BC.

2966 So, the reflection of point C over AB is point D.
 2967 So, to find the reflection of point C over AB, let's find the equation of AB first.

2969 Since A is at $(16,0)$ and B is at $(0,0)$, AB is the x-axis from $(0,0)$ to $(16,0)$.

2970 So, the line AB is $y=0$.
 2971 Reflecting a point over the x-axis changes the sign of the y-coordinate.

2970
 2971 So, the reflection of point C=(x,y) over AB (y=0) would be (x, -y).
 2972
 2973 But the reflection point is D, which is $(\frac{x}{2}, \frac{y}{2})$.
 2974
 2975 So, according to the reflection, $(x, -y)$ should equal $(\frac{x}{2}, \frac{y}{2})$.
 2976
 2977 Wait, that can't be unless $x = 0$ and $y = 0$, which would place C at the origin, but then ABC wouldn't
 2978 be a triangle.
 2979
 2980 **Hmm, that doesn't make sense.** Maybe my assumption that AB is the x-axis is causing confusion
 2981 because in reality, AB is just a chord, not necessarily the x-axis.
 2982
 2983 Alternatively, perhaps I should place AB as a horizontal chord but not necessarily aligned with the
 2984 x-axis.
 2985
 2986 Let me try that.
 2987
 2988 Let me place point A at (a, b) and point B at (c, d), but this might complicate things.
 2989
 2990 Maybe a better approach is to use coordinate geometry with AB as a chord, not necessarily aligned
 2991 with any axis.
 2992
 2993 Alternatively, maybe using vectors or geometric properties would be better.
 2994
 2995 Let's think about the reflection.
 2996
 2997 When you fold the arc AB over AB, point C is reflected over AB to point D on BC.
 2998
 2999 **... omitted**
 3000 When we fold arc AB over AB, the reflection of point C over AB is point D.
 3001
 3002 So, the reflection of C over AB is D.
 3003
 3004 Since AB is the x-axis from (0,0) to (a,0), the reflection over AB would invert the y-coordinate.
 3005
 3006 So, if C is at (x,y), then D would be at (x, -y).
 3007
 3008 But D is also the midpoint of BC, which is $(\frac{x_B+x_C}{2}, \frac{y_B+y_C}{2}) = (\frac{0+x}{2}, \frac{0+y}{2}) = (\frac{x}{2}, \frac{y}{2})$.
 3009
 3010 So, setting $(x, -y)$ equal to $(\frac{x}{2}, \frac{y}{2})$:
 3011 $x = x/2 \Rightarrow x = 0$
 3012
 3013 - $y = y/2 \Rightarrow -y = y/2 \Rightarrow -2y = y \Rightarrow 3y = 0 \Rightarrow y = 0$
 3014 Again, this leads to $y=0$, which would place C on AB, making ABC degenerate.
 3015
 3016 **Hmm, clearly, placing AB on the x-axis isn't working because it forces C to be on AB.** Let me try a
 3017 different approach without coordinate geometry.
 3018 Let me consider the properties of the reflection.
 3019
 3020 When we fold arc AB over AB, point C is reflected over AB to point D on BC.
 3021
 3022 So, AB is the perpendicular bisector of segment CD.
 3023
 3024 Therefore, AB is perpendicular to CD, and the midpoint of CD lies on AB.
 3025 Since D is the midpoint of BC, the midpoint M of CD is also the midpoint of BC, which is D itself.
 3026
 3027 So, D lies on AB and is the midpoint of CD.

3024 Therefore, AB is the perpendicular bisector of CD, so CD is perpendicular to AB, and D is the
 3025 midpoint of CD and lies on AB.
 3026 Wait, but D is also the midpoint of BC.
 3027
 3028 So, if D lies on AB, then BC must intersect AB at D, which is the midpoint of BC.
 3029
 3030 So, in triangle ABC, D is the midpoint of BC and lies on AB.
 3031
 3032 Therefore, AB is a median of the triangle, and since AB is also a side, it must be that triangle ABC is
 3033 such that AB is both a side and a median, which is only possible if ABC is an isosceles triangle with
 3034 $AB = AC$.
 3035
 3036 But the problem states $AB = BC = 16$, so if $AB = AC$, then it's an equilateral triangle, but in that case,
 3037 all sides would be 16, making $AC = 16$, but the answer seems to be $16\sqrt{2}$, so maybe that's not the
 3038 case.
 3039 **I'm really confused now.** Maybe the correct answer is $16\sqrt{2}$, as in the initial tentative solution, but
 3040 I'm not sure why.
 3041
 3042 Wait, another idea: since D is the midpoint of BC and lies on AB, and AB is a side, then ABC must
 3043 be such that AB is a median and an altitude, making it an isosceles triangle with $AB = AC$.
 3044
 3045 So, $AB = AC = 16$ exceeding maximum context length (8192)

3045
 3046
 3047
 3048
 3049
 3050
 3051
 3052
 3053
 3054
 3055
 3056
 3057
 3058
 3059
 3060
 3061
 3062
 3063
 3064
 3065
 3066
 3067
 3068
 3069
 3070
 3071
 3072
 3073
 3074
 3075
 3076
 3077